Global and Planetary Change 265 (2026) 105601

Contents lists available at ScienceDirect

Global and Planetary Change

journal homepage: www.elsevier.com/locate/gloplacha

Research Article

Climate–ocean changes across late Eocene-early Oligocene recorded at IODP Site U1553 (Southern Pacific Ocean)

Davide Righi [a], Valentina Catelli [a], Isabella Raffi [b], Chiara Fioroni [c], Giuliana Villa [a], Davide Persico [a,*]

[a] Dipartimento di Scienze Chimiche, della Vita e della Sostenibilità Ambientale - SCVSA, Università degli Studi di Parma, Parco Area delle Scienze 11/a, I-43124 Parma, Italy
[b] International Research School of Planetary Sciences - IRSPS, Università degli Studi "G. d'Annunzio" di Chieti-Pescara, Viale Pindaro 42, I-65127 Pescara, Italy
[c] Dipartimento di Scienze Chimiche e Geologiche, Università degli Studi di Modena e Reggio Emilia, Via G. Campi 103, I-41125 Modena, Italy

ARTICLE INFO

Editor: Dr. Fabienne Marret-Davies

Keywords:
Southern Ocean
Calcareous nannofossils
Eocene-Oligocene transition
Paleoecology
Paleoceanography
Paleoclimatology

ABSTRACT

We studied calcareous nannofossil assemblages from sediment cores of IODP Site U1553 (Campbell Plateau) for adding information on the environmental/climate context in this Southern Ocean region during the late Eocene-early Oligocene. The aim was to refine our understanding of conditions that led to the establishment of the permanent Antarctic ice sheet, through the study of a 5 million-years interval including the critical Eocene - Oligocene Transition (EOT). We performed a PCA to characterize the ecological preferences of counted species and used Temperate-Warm-Water Taxa index (TWWT index) and Eutrophic Index EI to delineate paleoenvironmental variability.

Our results provide evidence on the composition of the nannofossil assemblage for the effects of events preceding the EOT, such as a change chronologically coinciding with the effects of the Popigai meteor impact (at 36.63 Ma) and a transitional cooling interval around 34.6 Ma, which we term "Pre-LEE" (Pre-Late Eocene Event). Within the EOT (starting from ~34.46 Ma), the observed changes in nannofossil assemblage delineate a Temperate Transition Interval (TTI), an interstadial lasting from ~34.3 to ~34.2 Ma, during which temperate conditions prevailed. Through the studied interval, species diversity varies in three main phases, and assemblage-based SST and trophic indicators record a general decline in temperate and oligotrophic taxa and an increase in cool-water and eutrophic taxa.

The trend as delineated at Site U1553 shows differences with respect to other high southern latitudes sites, that seem to be related to the different paleoceanographic settings and, possibly, different paleobathymetry and paleotopography.

1. Introduction

The late Eocene - early Oligocene time is climatically characterized by a cooling trend that started in the middle Eocene (Kennett and Stott, 1990; Diester-Haass and Zahn, 1996). This post-MECO (Middle Eocene Climatic Optimum) trend set the stage for long-term global cooling during the middle and late Eocene (Zachos et al., 2001a, 2001b, 2008), along with changes in calcareous nannofossil assemblages (Villa et al., 2014). The migration of the proto-Ross Gyre and proto-Tasman Front (colder waters) (e.g., Nelson and Cooke, 2001; Huber et al., 2004) toward lower latitudes could explain the cooling that followed the Early Eocene Climatic Optimum (EECO) (Shepherd et al., 2021). In the late Eocene, the first notable climatic event was the Priabonian Oxygen Maximum (PrOM) (Scher et al., 2014), a brief cooling and/or ice sheet growth event (from 37.34 to 37.19 Ma) thought to derive from a glaciofluvial sediment transport system from Antarctic soils to the Southern Ocean (SO), which resulted in increased primary production and consequent cooling (Hutchinson et al., 2021). The PrOM is regarded as the initial phase of the Eocene-Oligocene Transition (EOT) (Scher et al., 2014). Subsequently, a Late Eocene event (LEE) was described by Katz et al. (2008) as characterized by a 0.5‰ increase in $\delta^{18}O$ in benthic foraminifera between 34.52 and 34.36 million years ago (Ma) (Coxall et al., 2005; Hutchinson et al., 2021). Few studies have documented this event in calcareous nannofossil records (Viganò et al., 2024; Viganò

* Corresponding author at: Department of Chemistry, Life Sciences and Environmental Sustainability, University of Parma, Italy.
E-mail address: davide.persico@unipr.it (D. Persico).

https://doi.org/10.1016/j.gloplacha.2026.105601
Received 10 February 2026; Received in revised form 16 June 2026; Accepted 29 June 2026
Available online 30 June 2026

and Agnini, 2025). The EOT (~34 Ma), marked the growth of the East Antarctic Ice Sheet (EAIS) (Tibbett et al., 2023) and its significant cooling had a fundamental impact on both marine and terrestrial ecosystems (Zachos et al., 2001a, 2001b; Coxall and Pearson, 2007; Westerhold et al., 2020; Hutchinson et al., 2021).

Two phases within the benthic foraminiferal stable oxygen isotope record characterized the EOT: the increase in $\delta^{18}O$ (EOT-1 or Step 1) reflecting seawater cooling (Coxall et al., 2005; Hutchinson et al., 2021) and the EOIS (Earliest Oligocene Isotope Step) related to ice growth (Katz et al., 2008; Bohaty et al., 2012; Hutchinson et al., 2021). Based on isotopic signals, the size of the ice sheet was estimated to be between 60% and 130% of its present mass (Lear et al., 2008).

Several studies also report an increase in $\delta^{13}C$ of about 0.5‰ in EOT benthic records (e.g., Zachos et al., 2001a, 2001b, 2008; Westerhold et al., 2020), due either to increased organic carbon burial in marine sediments associated with increased productivity in surface waters (Zachos and Kump, 2005), or to increased isotopically heavy carbon concentration related to enhanced erosion of neritic carbonates during marine regression (Merico et al., 2008). In addition to these isotopic shifts, notable changes include the rapid deepening of the carbonate compensation depth (CCD) (Coxall et al., 2005; Coxall and Pearson, 2007; Pälike et al., 2012; Taylor et al., 2023), the reduction of atmospheric pCO_2 (DeConto and Pollard, 2003), and sea level fall (Westerhold et al., 2020; Hutchinson et al., 2021; Tibbett et al., 2023).

The EOT was likely driven mainly by the gradual decrease in atmospheric pCO_2, a favourable combination of orbital parameters that favour ice preservation (Kennett et al., 1975; Coxall et al., 2005; Livermore et al., 2005; Pälike et al., 2006; Pagani et al., 2011; Hutchinson et al., 2021; Hönisch et al., 2023; Tibbett et al., 2023; Hochmuth et al., 2024), and the paleogeographic configuration of oceanic gateways (Abelson et al., 2008; Abelson and Erez, 2017; Coxall et al., 2018; Hutchinson et al., 2019; Straume et al., 2020; Hutchinson et al., 2021; Straume et al., 2022).

Looking at the various paleobathymetric models and proxies reported in the literature, there are different opinions and hypotheses on the evolution and the timing of closure and opening of ocean gateways (e.g., Rebesco et al., 2014). Straume et al. (2022) hypothesize that bathymetric changes in the Greenland-Scotland Ridge (GSR) and the presence of a shallow proto-Fram Strait facilitated the cooling of the Southern Hemisphere more than the SO passages and the possible initial closure of the Tethys Seaway. Coxall et al. (2018) point out that the North Component Water (NCW), precursor of the North Atlantic Deep Water (NADW) and part of the Atlantic Meridional Overturning Circulation (AMOC), could have affected heat transport at both poles. In contrast, Scher et al. (2011) report that the source of non-radiogenic εNd values during the first $\delta^{18}O$ step at ODP Site 738 was probably closer to the Kerguelen Plateau than Agulhas Ridge, which contradicts the hypothesis that the isotopic excursion is due to the influx of NCW.

The Antarctic Circumpolar Current (ACC) began roughly 31 million years ago (Scher et al., 2015; Hodel et al., 2021) and is a part of the AMOC (Borrelli et al., 2014). Its development was linked to the opening of the Drake Passage after the EECO (Straume et al., 2020; Hodel et al., 2022) and the Tasmanian Seaway after the MECO. The deepening of the ACC was estimated to occur between the late Eocene (Houben et al., 2019; Hodel et al., 2022) and the early Oligocene, notably, approximately between 35 and 31 million years ago (Hodel et al., 2021).

The replacement of illite and chlorite with smectite at ODP Site 689 sediment record (Wei et al., 1992), and the simultaneous occurrence of ice-rafted debris (IRD), biosilica-rich nannofossil muds, fish skeletal debris, and glauconite at ODP Site 748B (Wei et al., 1992), support changes in the patterns or intensity of ocean circulation (upwelling) that were linked to significant climatic cooling. Furthermore, a peak in IRD coarse sand (>425 μm) recorded at ODP Site 738, together with fossil fish tooth εNd excursion slightly before IRD deposition, are thought to be related to ice sheet expansion (Scher et al., 2011). As for the increase in opal concentration, due to increased eutrophication, it varied at different locations: at ODP Site 1090B it was generally weak before the EOT and grew, with a rise of over 15%, after the EOT (Salamy and Zachos, 1999). In contrast, at ODP Site 689D, three peaks in opal concentration are observed, at the Eocene/Oligocene boundary, during the middle-early Oligocene, and at the early-late Oligocene boundary, separated by periods of increased carbonate sedimentation (Diester-Haass, 1991). Around the EOT and the Oi-1 glaciation (Miller et al., 1991) at the start of the EOGM (Early Oligocene Glacial Maximum) (e.g., Zachos et al., 1992; Liu et al., 2004; Bohaty et al., 2012; Hutchinson et al., 2021), a 90% to 60% reduction in $CaCO_3$ was detected, as at ODP Site 744 A (Barker et al., 1988; Jones et al., 2019) and an increase of 4% to 8% in SiO_2 (Diester-Haass, 1991). According to Hutchinson et al. (2021), the end of the EOT marks the start of the EOGM, while Zachos et al. (1996) associate the EOGM with the Oi-1 event (Zachos et al., 1992) and the permanent glaciation of East Antarctica that occurred at about 33.7 million years ago (e.g., Zachos et al., 2001a, 2001b; Bohaty et al., 2012; Hutchinson et al., 2021).

This study deals with the late Eocene - earliest Oligocene calcareous nannofossil assemblages from sediment cores of IODP Site U1553 located in the southern Pacific Ocean and aims to verify the ecological preferences of the observed taxa during this critical time interval.

We compare the obtained results with previous studies in coeval deep-sea sediment successions located at high southern paleolatitudes (Persico and Villa, 2004; Villa et al., 2008; Villa et al., 2014) in an effort of providing a wide-ranging analysis of the response of calcareous nannoplankton to the EOT in the Southern Ocean.

2. Material and methods

2.1. IODP Site U1553 and Southern Ocean sections

During IODP Expedition 378 (South Pacific Ocean, Campbell Plateau; Thomas et al., 2018; Röhl et al., 2022), five holes (A, B, C, D, and E) were drilled at a single Site U1553, reaching a maximum depth of 584.3 CCSF m, and a ~ 581 m-thick sedimentary section was recovered comprising Pleistocene to Paleocene deep-sea sediments. A composite sedimentary section was obtained splicing cores from A, B, and E holes (Drury et al., 2022), and this study covers a ~ 79 m-portion of it (from 263.81 to 184.78 CCSF m) that corresponds to the late Eocene - early Oligocene stratigraphic interval (biozones NP18 - NP21). The previously published high-resolution biostratigraphic study of calcareous nannofossils in the same interval (Raffi et al., 2024) provided the age-depth model used here. This chronology is the only one available for Site U1553 in the late Eocene-early Oligocene in the absence of a specific stable isotope and magnetostratigraphic record. It derives from the updated biochronology of SO nannofossils obtained through correlation with reference magnetostratigraphic and stable isotope records (Fioroni et al., 2015; Villa et al., 2008; Persico and Villa, 2004). The bioevents in Raffi et al., 2024 have been converted to GTS2020. Therefore, the reliability of the employed model is inevitably affected.

We compare the results obtained at Site U1553 with results from other reference deep-sea sections located in the SO (ODP Sites 738, 748, 744 in the Kerguelen Plateau; ODP Site 689 in the Maud Rise) and Southern Atlantic (ODP Site 1090 in the Agulhas Ridge) (data by Persico and Villa, 2004; Villa et al., 2008; Pea, 2011).

2.2. Calcareous nannofossil data

We conducted the quantitative analysis on 809 samples, using a Zeiss AxioSkop 2 microscope with 1250× magnification. Sample resolution varies through the studied section: sampling intervals are 6–10 cm in the interval from 192.18 to 184.78 CCSF and from 197.85 to 263.81 CCSF, and 3–5 cm from 192.26 to 197.77 CCSF. Samples were prepared according to the standard "smear slide" technique of Bown and Young (1998). The significant taxa are represented in Plate 1. The impact of reworking in the surroundings of the EOT is negligible compared to the

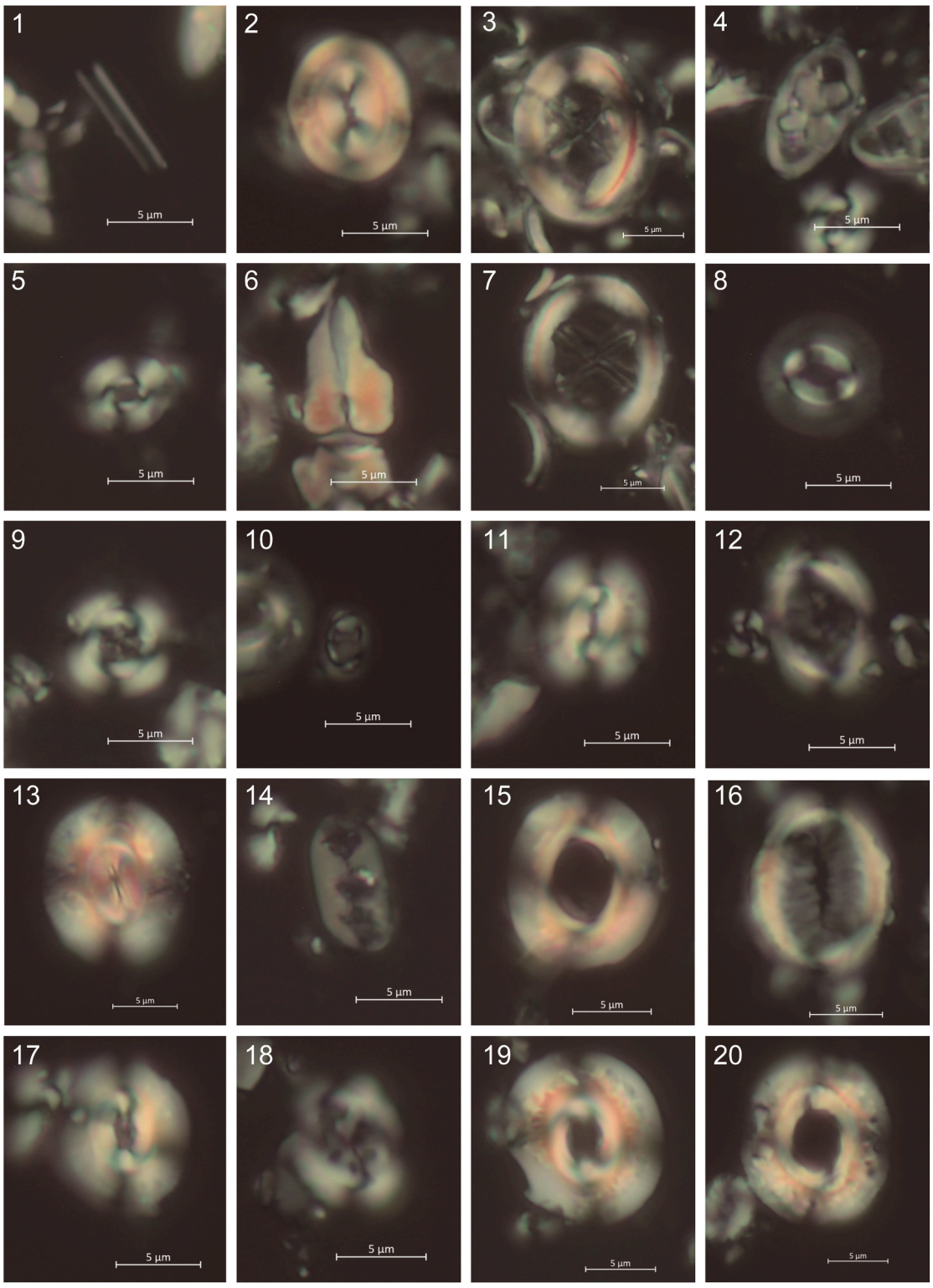

Plate 1. : LM microphotographs of selected calcareous nannofossils from IODP Site U1553, all specimens at 1250× magnification. 1. *Blackites* sp., crossed nicols, U1553A-24-1, 120–121; 2. *Bicolumnus ovatus*, crossed nicols, U1553B-22-1, 137–138; 3. *Chiasmolithus eoaltus*, crossed nicols, U1553B-22-1, 101–102; 4. *Neococcolithes dubius*, crossed nicols, U1553B-29-3, 94–95; 5. *Cyclicargolithus floridanus*, crossed nicols, U1553A-24-1, 120–121; 6. *Zygrhablithus bijugatus*, crossed nicols, U1553A-24-1, 120–121; 7. *Chiasmolithus oamaruensis*, crossed nicols, U1553A-24-1, 20–21; 8. *Coccolithus pelagicus*, crossed nicols, U1553A-24-1, 120–121; 9. *Cribrocentrum reticulatum*, crossed nicols, U1553B-28-2, 46–47; 10. *Clausicoccus subdistichus*, crossed nicols, U1553E-20-3, 22–23; 11. *Dictyococcites bisectus*, crossed nicols, U1553A-24-1, 120–121; 12. *Reticulofenestra clatrata*, crossed nicols, U1553B-29-3, 94–95; 13. *Dictyococcites stavensis*, crossed nicols, U1553A-24-1, 20–21; 14. *Isthmolithus recurvus*, crossed nicols, U1553A-24-1, 20–21; 15. *Reticulofenestra umbilicus*, crossed nicols, U1553A-24-1, 120–121; 16. *Reticulofenestra* cf. *oamaruensis* (10–12 µm), crossed nicols, U1553B-22-1, 137–138; 17. *Reticulofenestra filewiczii*, crossed nicols, U1553B-22-1, 137–138; 18. *Reticulofenestra daviesii*, crossed nicols, U1553A-24-1, 120–121; 19. *Reticulofenestra hillae*, crossed nicols, U1553A-24-1, 120–121; 20. *Reticulofenestra samodurovi*, crossed nicols, U1553A-24-1, 120–121.

overall abundance of the association per sample. Preservation is good throughout the interval. There is a decrease in preservation in the surroundings of the EOT (good to moderate), and does not compromise the results (Raffi et al., 2024). Nannofossil preservation was assessed as good (G) to moderate (M) using the scale of Bown and Young (1998). To have a reliable representation of the calcareous nannofossil assemblage, 500 specimens in each sample were counted and identified, selecting specimens with more than half of intact structure, and the relative percentages of taxa within assemblage were obtained. The abundance data, recorded using BugWin 2020 software, were subsequently exported to an Excel spreadsheet and converted from absolute specimen abundance/Field of view (FOV) to absolute abundance/mm^2 per sample to obtain estimate suitable for statistical purposes. To reduce the dataset specific variability to a few factors (components), we conducted a PCA (Principal Component Analysis) on the variance-covariance matrix (Q-Mode) using Past 4.16c (Hammer et al., 2001). Relative abundances were normalised with respect to variance-covariance, and reworked species were removed from the database used for statistical analyses. The data were then linearly transformed using the "log10" function to ensure equal statistical weighting of abundance values of different orders of magnitude and to ensure that the new variables obtained (PCA axes) were linear.

Below we report the taxonomic groupings proposed to reduce potential errors caused by incorrect systematic classification, that are shown in Table 2.

According to Nannotax3 (Young et al., 2024), we considered three "morphogroups" within the genus *Reticulofenestra* differentiated by the structure of their central areas, as follows: i) the *Reticulofenestra umbilicus* group, in which we included *R. umbilicus*, *R. samodurovi*, *R. hillae*, *R. dictyoda*, and excluded *R. oamaruensis* and *R. clatrata* (= *R. onusta* sensu Wei et al., 1992), that have been considered separately for investigating in detail their paleoecological preferences; ii) the *R. oamaruensis* group, that includes *R. oamaruensis* ($\geq$ 14 μm in size) and *Reticulofenestra* cf. *oamaruensis* ($<$ 14 μm); iii) the *R. lockeri* group here represented by a single species, the *R. daviesii.* We considered the genus *Dictyococcites* as a separate taxonomic unit from *Reticulofenestra* (in agreement with Agnini et al., 2014; Viganò et al., 2023). This group includes *D. bisectus*, *D. scrippsae*, *D. stavensis*, *R. perplexa* and *R. filewiczii*.

Following the same approach, the other morphogroups / species considered are listed below:

- *Chiasmolithus* spp. (*C. bidens* gr. + *C. consuetus* gr.), including *C. solitus*, *C. oamaruensis*, *C. eoaltus*, *C. altus*, *C. nitidus* and *C. consuetus*;
- *Coccolithus pelagicus* group, including *C. pelagicus* and *C. eopelagicus*;
- *Cribrocentrum reticulatum* group, including *C. reticulatum*, *C. westerholdii*, *C. isabellae*, and *C. erbae*;
- *Neococcolithes dubius*;
- *Blackites spinosus* group, including *Blackites spinosus*, *B. stilus* and *Blackites*. spp.;
- *Clausicoccus subdistichus* group, including *C. subdistichus*, *C. fenestratus* and *Clausicoccus* spp.;
- *Cyclicargolithus floridanus*;
- *Bicolumnus ovatus*;
- *Zygrhablithus bijugatus*.

Paleoenvironmental significance of PC1 and PC2 was evaluated by comparing them with independent paleoclimate proxies from ODP 689D (δ^{18}O and δ^{13}C) because are not available for Site U1553. Based on the PCA' results, compared with paleoecological groupings from previous works (Villa et al., 2014), we calculated the Eutrophic Index = (eutrophic-water taxa/(eutrophic-water taxa+oligotrophic-water taxa+mesotrophic-water taxa))*100]) (EI) (Catelli et al., 2025) and the TWWT index (Temperate-Warm-Water Taxa = [(temperate-water taxa) / (temperate-water taxa + cool-water taxa))*100] (Villa et al., 2008), with the aim of better delineating the variability in paleoceanographic conditions. In addition, the taxa relative percentages were summed based on the established ecological preferences to interpret trends. We computed the Shannon index (H′) to highlight changes in species richness over time (Shannon and Weaver, 1949). Finally, we compared the results with data from other SO Sites 748B (Villa et al., 2008), 738B (Our data), 744A and 689D (Persico and Villa, 2004) and from the mid-paleolatitude Site 1090B (Pea, 2011) to formulate a broader interpretation.

2.3. Geological features and paleoceanographic settings

It is well known that oceanic currents, paleolatitude, and biogeographic isolation are the most important factors in regulating the relationship between nannofossil distribution and water masses (e.g. Viganò et al., 2024). To demonstrate the possible oceanic-currents configuration of the SO region including Site U1553 and the other ODP sites considered in this study, we reconstructed the paleobathymetry, paleotopography, and paleocoordinates (Fig.1), using data from Straume et al. (2023) and the rotational model of Torsvik et al. (2019) with the software R 4.3.3, Qgis 3.38.0, and Gplates 2.4.0. These details and data on the interaction between ocean circulation and topography can help in explaining signals and variability recorded in our records: for instance, there is evidence that underwater reliefs such as Maud Rise or Kerguelen Plateau induce cold, nutrient-rich water to rise (Diester-Haass and Faul, 2019). The influence of the Kerguelen Plateau's topography on the ACC was recently proposed (Diester-Haass and Faul, 2019). As regards the previously depicted paleoceanographic setting of the area in the time interval considered in this study (from 37.95 to 33.058 Ma), it is evident that the oceanic circulation patterns were broadly similar to today, with the exception of the presence of a "proto-ACC" (Fig.1).

3. Results and discussion

Since the following interpretations lack proxies that would definitively corroborate the trends identified, they are included in a theoretical paleoceanographic framework that is nonetheless supported by the existing literature.

3.1. Ecological preferences of calcareous nannofossils

The results of PCA conducted on nannofossil assemblages provided hints on the paleoecological structure of the Upper Photic Zone (UPZ) in the South Pacific Ocean during the late Eocene - early Oligocene and on the evolution of the Trophic Resource Continuum (TRC), that could have been involved in the extinction of some taxa, the regulation of species dominance, and in the selection of certain morphological features over others (Hallock, 1987). The total variance of our dataset is approximately 62.4%, with 46.52% (PC1) and 15.88% (PC2), identified in the present study such as trophic conditions and sea surface temperature (SST), respectively (Fig. 2 A and 2 B). The other components represent "background noise". The loadings values of the analysis are shown in Fig. 2 C. The significant positive autocorrelation detected in the PCA scores indicates that the observed assemblage changes are stratigraphically structured rather than random (PC1: Moran's $I = 0.708$, $p < 0.05$; PC2: Moran's $I = 0.659$, $p < 0.05$). Although autocorrelation alone does not demonstrate that the ordination axes represent meaningful ecological gradients, the Broken Stick Model supports the retention of the first two axes. Both PCs account for a greater proportion of variance than expected under a random distribution. Together, these axes explain more than 50% of the total variance, supporting their interpretation as major paleoecological gradients rather than artefacts of temporal dependence. The attribution of the paleoecological charaterizaction was realized by the correlation of the paleoecological behaviour of the species recorded in other sites (e.g., Villa et al., 2008; Villa et al., 2014; Viganò et al., 2023).

Coccolithophores are considered eurythermic organisms (e.g. Viganò

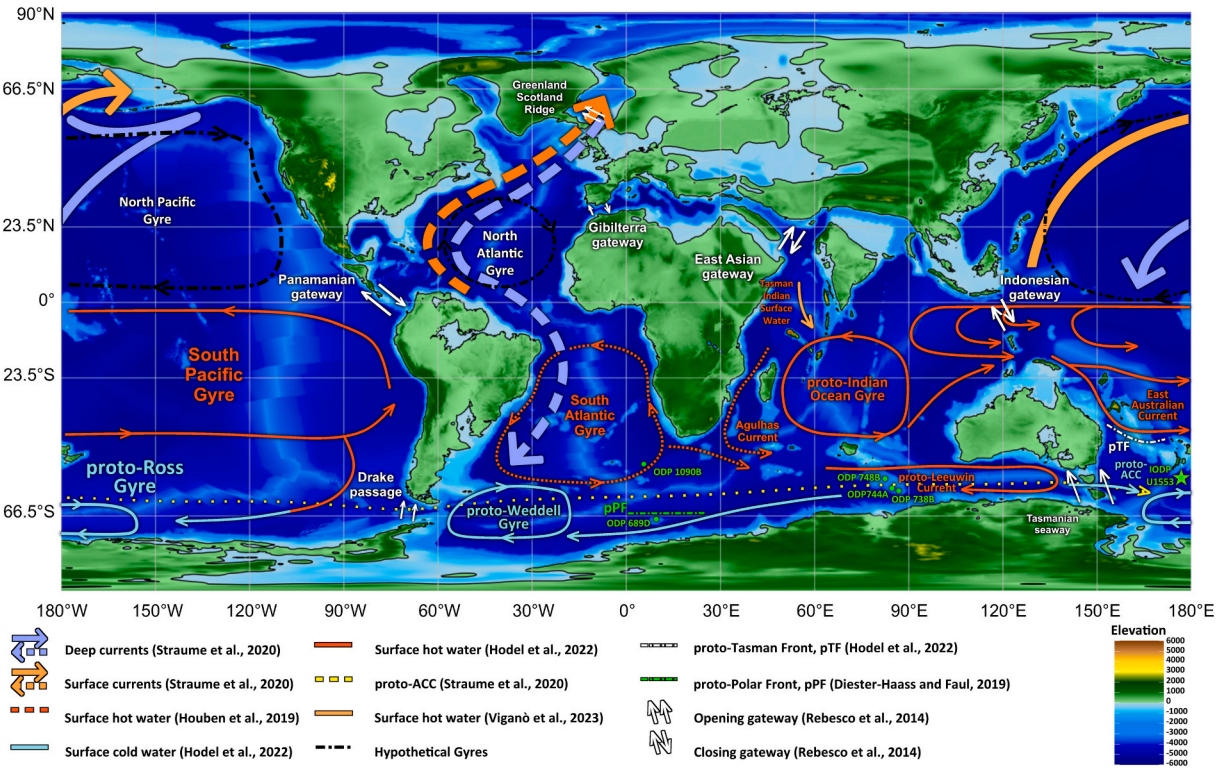

Fig. 1. Global paleogeographic map, with topography and bathymetry at 34 Ma, generated with data by Straume et al. (2023) and rotational model of Torsvik et al. (2019) using R 4.3.3 (packages "ncdf4", "ggplot2", "scales" and "grid"), Qgis 3.38.0 and Gplates 2.4.0. Included is a paleoceanographic reconstruction, with tracks of paleocurrents in the Southern and Northern Hemisphere at 34 Ma, based on paleoceanographic data from the literature. Different lines and colours indicate the types of currents (cold, warm, deep and surface) and openings/closings of oceanic gateways. Green star = IODP Site U1553; green dots = ODP Sites used for discussion. (For interpretation of the references to colour in this figure legend, the reader is referred to the web version of this article.)

et al., 2023), but numerous studies have shown that they have specific ecological preferences (Villa et al., 2008; Cappelli et al., 2021; Viganò et al., 2024; Sheward et al., 2024). Nutrient concentration, temperature, and salinity are among the factors that most influence nannoplankton/nannofossil distribution (Villa et al., 2014). Calcareous nannoplankton is typically better adapted to oligotrophic conditions, although some species exhibit a preference for eutrophic conditions (Brand, 1994; Ziveri et al., 2004; Villa et al., 2014). Starting from these general ecological preferences inferred for nannoplankton/nannofossils and known from the literature, we defined the "ecological" groups reported in Table 2, that have the ecological preferences revealed from our analysis, as discussed below.

- *Coccolithus pelagicus* gr.: This taxon seems to have changed its temperature preference over time, showing a progressive trend toward colder climates through its long stratigraphic range (Wei and Wise Jr., 1990). Previously reported preferences for *C. pelagicus* include, temperate (Persico and Villa, 2004; Villa and Persico, 2006; Villa et al., 2008; Villa et al., 2014), warm (Viganò et al., 2023), or temperate to-cold conditions (Demircan and Yıldız, 2007). Our PCA' data highlight a preference for temperate and eutrophic conditions, according to Villa et al. (2014).
- *Cyclicargolithus floridanus*: It is considered a cosmopolitan (Wei and Wise Jr., 1990), temperate (Lasluisa et al., 2024) and eutrophic taxon (Aubry, 1992; Monechi et al., 2000; Dunkley Jones et al., 2008; Fioroni et al., 2015; Villa et al., 2021). In this study, the correlation with the PC1 curve suggested revising the paleoecological interpretation of the species by classifying it as mesotrophic.
- *Dictyococcites bisectus* gr.: As reported in the literature, *Dictyococcites* species show strongly contrasting environmental preferences that probably reflect species-specific responses to environmental factors, even if taxonomic uncertainties cannot be ruled out. This uncertainty in differentiating the ecologic preferences of the various species could be also related to the difficulty in discerning the complex network of interactions within the marine ecosystem (Viganò et al., 2023). In line with this problem, our PCA' results suggest for this morphogroup a mesotrophic/temperate character, whereas in the literature it is considered a warm-temperate (Wei and Wise Jr., 1990), warm (Monechi et al., 2000), temperate (Wei et al., 1992; Persico and Villa, 2004; Persico and Villa, 2004; Villa et al., 2008), temperate-eutrophic (Villa et al., 2014), or cool-eutrophic (Sheward et al., 2024) taxon.
- *Isthmolithus recurvus*: The ecologic preferences of this species have been variably described so it sometimes has been controversially classified as a temperate (Persico and Villa, 2004; Villa et al., 2008; Villa et al., 2014), or cool (Wei et al., 1992; Monechi et al., 2000), or warm/oligotrophic (Viganò et al., 2023) or eutrophic (Sheward et al., 2024) taxon. PC1 and PC2 resultsseem to indicate a temperate-eutrophic preference for it.
- *Reticulofenestra*: The species and morphogroups referred to this genus exhibit different ecological preferences, that seem related to water temperature and trophic conditions. According to several authors (Monechi et al., 2000; Villa et al., 2014; Fioroni et al., 2015; Villa et al., 2021; Sheward et al., 2024; Viganò et al., 2024), *Reticulofenestra daviesii* had eutrophic and cold-water preferences considering PC1 and PC2. The *Reticulofenestra umbilicus* gr. includes species considered eutrophic taxa (Villa et al., 2014, 2021; Sheward et al., 2024), or species that have a temperate-water preference (Wei and Wise Jr., 1990; Persico and Villa, 2004; Villa et al., 2008, 2014) as our PCA results suggest. As regards the ecology of *Reticulofenestra clatrata*, there are no indications from previous studies, probably because the taxon went previously unnoticed due to its low abundance or it was included in a morphogroup. Our PCA' data suggest that *R. clatrata* is a temperate and mesotrophic taxon. Very few are

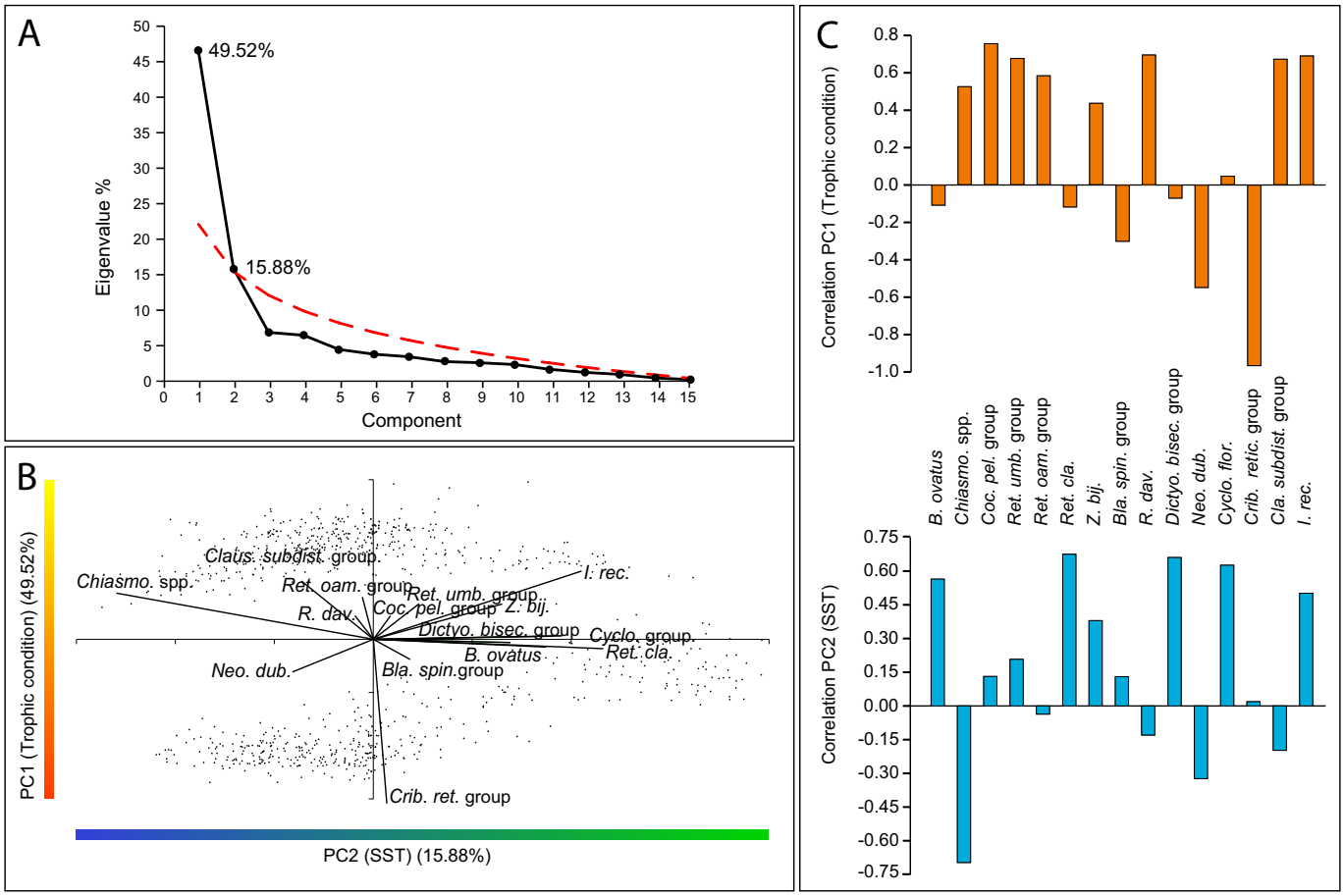

Fig. 2. PCA results from IODP U1553. (A) Scree plot of principal components; (B) PCA scatter plot; (C) correlation loadings values for PC1 (Trophic conditions) and PC2 (SST).

the references in the literature to the paleoecology of *Reticulofenestra oamaruensis* that was considered as a cool-water taxon (Monechi et al., 2000) whereas we regard it as a temperate and eutrophic taxon instead. Note that our observations on the ecologic preferences of *R. clatrata* and *R. oamaruensis* are consistent with the paleoceanographic dynamics inferred from the obtained results (Figs. 3 A and 3 B). In another study on Site U1553 (Catelli et al., 2025), we suggested that the morphotypes of *R. oamaruensis* occurred under the eutrophic conditions established through a "trophic switch", in line with the eutrophic character inferred for this taxon by Villa et al. (2014). The temperate taxa *R. clatrata* and *R. oamaruensis* concomitantly became extinct during the EOT (Fioroni et al., 2015; Raffi et al., 2024; Sheward et al., 2024) when a reduced SST regime began to prevail.

- *Clausicoccus subdistichus* gr.: Observing PC1 and PC2, we consider this taxon as cold-eutrophic, in agreement with Fioroni et al. (2015) and Viganò et al. (2024).
- *Chiasmolithus* spp.: The ecologic preferences suggested for this taxon vary from temperate or temperate-cold (e.g., Fioroni et al., 2015; Viganò et al., 2023), to cold conditions (Wei et al., 1992; Villa et al., 2014; Sheward et al., 2024; Viganò et al., 2024). It has been also considered a eutrophic taxon (Wei et al., 1992; Bralower, 2002; Villa et al., 2014; Fioroni et al., 2015; Viganò et al., 2023; Sheward et al., 2024; Viganò et al., 2024). Our PCA' results suggest that *Chiasmolithus* spp. preferred cool-water and eutrophic conditions.
- *Neococcolithes dubius*: Although this species is considered an oligotrophic (Bindiu-Haitonic et al., 2021) and temperate-water taxon (Villa et al., 2008), our PCA' results suggest that it was a cool-water taxon adapted to oligotrophic conditions.
- *Cribrocentrum reticulatum* gr.: Our PCA' data indicate that this taxon had preference for oligotrophic and temperate conditions, in line with previous findings (Villa et al., 2008, 2014; Fioroni et al., 2015).
- *Blackites spinosus* gr.: Our PCA' results suggest a preference for oligotrophic and temperate conditions for this taxon, even though previous studies indicated it as a mesotrophic form more adapted to cool waters (Sheward et al., 2024; Kochhann et al., 2021).
- *Zygrhablithus bijugatus:* Many conflicting opinions are reported in the literature on the paleoecologic preferences of this taxon. Based on our PCA' data the species seems to have eutrophic and temperate-water preferences, in agreement with Villa et al. (2008) who suggested it could be a temperate taxon.
- *Bicolumnus ovatus*: Our PCA' results suggest that this taxon had preference for temperate and mesotrophic water. It is noteworthy that the lack of a paleoecological characterization for this species in previous studies on EOT (e.g., Villa et al., 2008; Fioroni et al., 2015; Villa et al., 2021; Viganò et al., 2023) could be due to its sporadic presence in those records, while in the studied section it shows a continuous distribution range, with peaks in abundance reaching ~90 specimens/mm^2.

3.2. Paleoceanography and paleoclimatology

The paleoceanographic reconstruction of Fig. 1 shows the surface currents that influenced Site U1553 around 34 million years ago, mainly delineated by a proto-ACC (cold waters) and a proto-Ross Gyre (cold waters) (Straume et al., 2020; Hodel et al., 2022). The presence of a proto-Tasman Front could have limited the arrival of warm waters brought by the East Australian Current (EAC) (Fig. 1) (Hodel et al.,

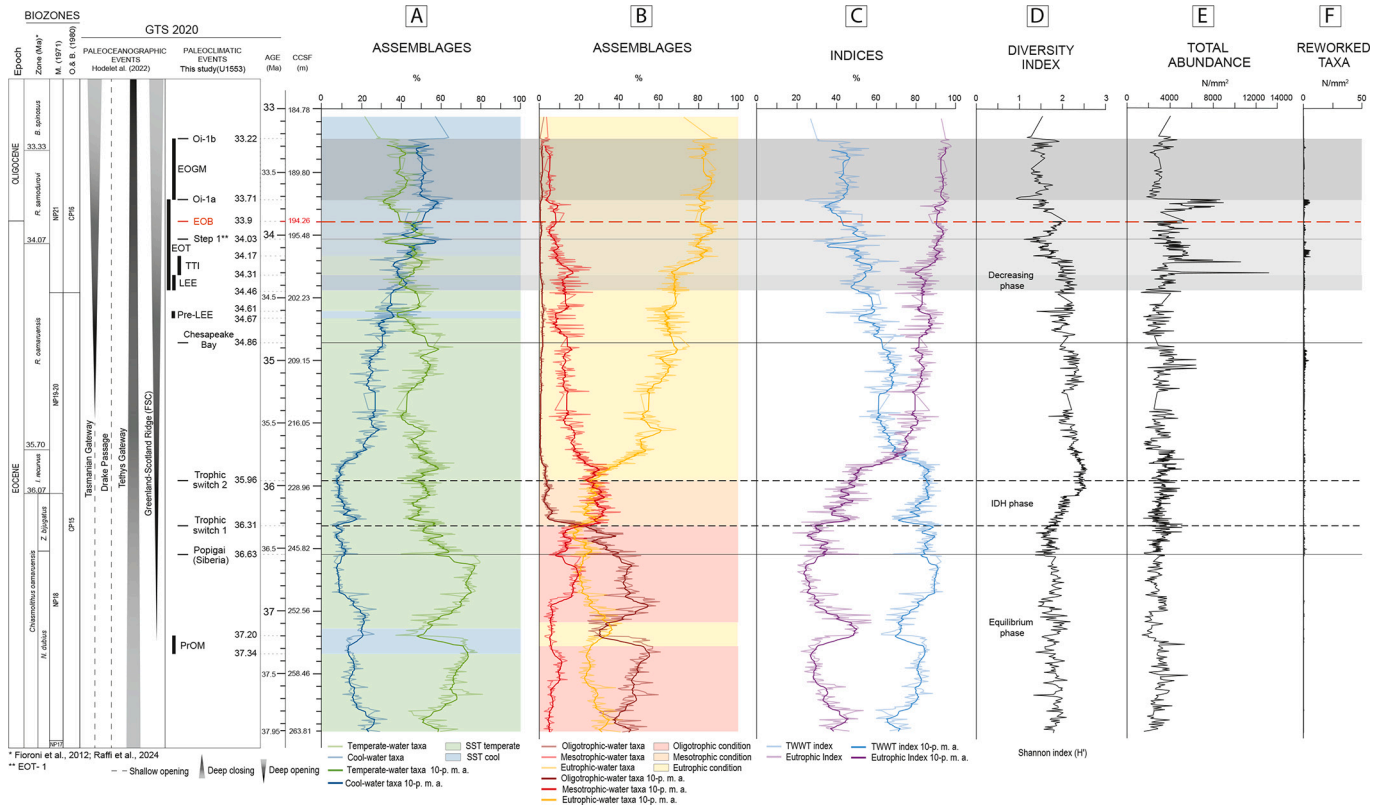

Fig. 3. Data on calcareous nannofossil assemblages, showing variability related to changes in temperature and trophic conditions in the studied interval at IODP Site U1553. (A) variability in the relative abundance records of temperate-water and cool-water taxa, clustered based on SST (Sea Surface Temperature); (B) variability in the relative abundance records of oligotrophic-, mesotrophic- and eutrophic-taxa, clustered based on trophic conditions. Major paleoclimate, geological, and paleoceanographic events of the late Eocene - early Oligocene are shown to the left with, chronostratigraphy, biostratigraphy and age. Biostratigraphic scheme from Fioroni et al. (2015) compared to the standard zonations of Martini (1970) and Okada and Bukry (1980). The grey shaded areas correspond to the EOGM, EOT, and LEE intervals. The dotted red horizontal line marks the E/O boundary; the dotted grey horizontal lines mark the Trophic switches 1 and 2; the solid lines indicate the meteor impacts of Popigai and Chesapeake Bay. (A) taxa-group (%) based on SST (Sea Surface Temperature); green lines and intervals = temperate taxa/conditions; blue lines and intervals = cold taxa/conditions. (B) abundance (%) of taxa-groupings based on trophic conditions, yellow intervals = eutrophic taxa/conditions; orange lines and intervals = mesotrophic taxa/conditions; red lines and intervals = oligotrophic taxa/conditions. (C) Compared records of TWWT index (blue) and EI (red). (D) Diversity record (Shannon-Weaver index H′). (E) Nannofossil total abundance (specimens/mm^2). (F) Reworked specimens (specimens/mm2). (For interpretation of the references to colour in this figure legend, the reader is referred to the web version of this article.)

2022).

The paleoposition of Site U1553, to the East of the Tasmanian seaway, is strategic for a detailed description of paleoceanographic dynamics in the Australia-New Zealand region. According to Diester-Haass and Faul (2019), during the EOT the proto-Polar Front was consistently positioned close to the Maud Rise, as shown in our reconstruction (Fig. 1). Sheward et al. (2024) report that nannofossil assemblage data from this same Site U1553, together with biogenic and geochemical proxies from different studies, are consistent with a paleoposition located further north of the proto-Subantarctic Front (proto-SAF), which, however, appears to have migrated northwards. Pascher et al. (2015) and Hodel et al. (2022) report a significant abundance increase of diatoms and radiolarians at DSDP Site 277 (that was at the same location of Site U1553), related to the presence of colder and more nutrient-rich waters, between ~35.3 and 32.4 Ma. In the sub-Antarctic region, at the opening of Tasman seaway and Drake passage and the subsequent development of the proto-ACC, the position and strength of the proto-Subtropical Front (proto-STF) and related currents should have been influenced, thus determining upwelling regimes at mid and high latitudes (Sheward et al., 2024). Shepherd et al. (2021) suggested that a shift toward low latitudes of the cold water proto-Tasman Front and proto-Ross Gyre could explain the post-EECO cooling trend.

After reconstructing the geological and oceanographic context of the study area and defining the ecological preferences of the taxa, we analysed the abundance distributions of individual ecological groups. The TWWT and EI indices, within the age-depth model proposed by Raffi et al. (2024), were used to reconstruct a plausible scenario for the evolution of SST and trophic conditions. Two trophic switches ("Trophic switch 1" and "Trophic switch 2"; see below) were proposed through the new statistical investigation conducted on Site U1553, delineating in more detail the passage from oligotrophic to eutrophic conditions around ~36.53 Ma, previously suggested by Catelli et al. (2025). The records obtained are shown in Fig. 3 in which we compare our data with the major paleoclimate, geological, and paleoceanographic events of the late Eocene - early Oligocene correlated with data from IODP Site U1553. These records suggest a potential paleoecological evolution in this sedimentary section and hint at a sequence of different ecological regimes through a ~ 5 million-years interval.

The trends observed in the taxonomic groups are considered more functional for discussion than trends of individual species, because they reduce the potential errors in counting, limit the effects of specimen preservation, and restrain control exerted by evolution (Wei and Wise Jr., 1990). Stable isotope oxygen and carbon records are not yet available, preventing a thorough comparison of our data with these other proxies.

3.2.1. *Nannofossils and paleotemperature (SST)*

As shown by the % assemblages records obtained through the studied section (Fig. 3 A), temperate-water taxa and cool-water taxa are negatively correlated ($r = -0.643$). In this 5 million-years interval the degree

of variability within nannofossil assemblages appears to have changed in response to the evolving climate/environment, suggesting that different intervals appear can be distinguishable and described hereinafter.

3.2.1.1. Changes in the Late Eocene. At the base of the studied section, across a ~ 600 Kyr-interval, temperate-water taxa reach a maximum of ~75–80% and cool-water taxa of ~20–25% (TWWT index min. = ~59%, max. = ~89%). This trend is interrupted around the PrOM (from 37.34 to 37.19 Ma), when the temperate-water taxa decrease from ~80% to ~40%, the cool-water taxa increase by ~10%, and the TWWT index decreases from ~89% to ~60%. These changes represent a climatic event that was previously reported in the Kerguelen Plateau as the "Middle/late Eocene cooling event C" by Villa et al. (2008) and successively confirmed by Scher et al. (2014). It was suggested that this cooling could have caused the stratification of the water column with a subsequent nutrient depletion in the photic zone and an increase of the Ocean Biological Pump (OBP) in sequestering carbon (Villa et al., 2014). Starting from ~37 Ma, temperate-water taxa reach a maximum of ~79% and a minimum of ~43%, while cool-water taxa reach a maximum of ~25% and a minimum of ~5% (TWWT index = min. ~63% and max. ~92%). Around 36.63 Ma, the Popigai meteor impact occurred (Masaitis et al., 1971; age recalibration by Schmieder and Kring, 2020). The stratigraphic evidence of this impact in the southern hemisphere was recorded at SO sections located at similar latitudes to Site U1553 as ODP Sites 1090B and 738B (Liu et al., 2009) and Antarctica ODP Site 689 (Coccioni et al., 2000), in which the co-presence of an Ir anomaly, a clinopyroxene (cpx) spherule layer, and a decrease of approximately 0.5‰ in $\delta^{13}C$ were observed. The decrease of $\delta^{13}C$ was explained as due to a cooling phase with increase in water nutrients (Passchier et al., 2017; Jones et al., 2019). The reason why these sediment features were not recorded in U1553 could be explained by the reconstruction of the cpx strewn field and pattern of deposition (Wrobel and Schultz, 2003), from which it appears that U1553 is outside the deposition trajectory, while the nearby DSDP Site 592 is located inside and has the cpx spherule layer in its record.

In this study, we recorded a significant decrease in temperate-water taxa (from ~80% to ~40%) and a decrease of oligotrophic-water taxa (from ~50% to ~25%) in the interval coeval to the Popigai impact (Fig. 3 A, B; Fig. 4 a, b). The concomitant pointed decrease in the TWWT index (from ~90% to ~70%) and increase in EI (from ~25% to ~50%) (Fig. 3 C) are consistent with the result of Passchier et al. (2017) and could reflect an evolutionary change in plankton due to this impact, as inferred by Montanari and Koeberl (2000). The transition from oligotrophic to mesotrophic conditions, that potentially gradually initiated at the Popigai impact event, proceeded above, delineating the "Trophic switch 1" (Fig. 3 B): the TWWT index decreased from ~90 to ~70% and then recovered to ~90% (Fig. 3 C), shortly after the "Trophic switch 2", when cool-water taxa abundance varied from ~5% to ~20% and temperate-water taxa abundance from ~60% to ~40%. Once eutrophic conditions were established, a sharp increase of cool-water taxa from ~10% to ~40% was recorded together with a change of the TWWT index from ~90% to ~60%. These paleoecological variations appear to be coeval with the Popigai event, however, due to the absence of direct evidence for an impact-related signal at Site U1553, a causal relationship cannot be established.

3.2.1.2. Changes at the EOT. The increasing trend in cool-water taxa, observed from the "Trophic switch 2" upwards, culminates in the EOT-1 interval, also referred as Step 1 (Scher et al., 2011; Hutchinson et al., 2021) or Oi-1a and Oi-1b (Zachos et al., 1996). Accordingly, from ~35.85 Ma upwards the TWWT index showed a decreasing trend (Fig. 3 C). In the preceding ~600 Kyr-interval, the values were slightly increasing, then decreased from values of ~90% to values of ~30% at Step 1 (Scher et al., 2011; Hutchinson et al., 2021), ~24% at Oi-1a (Zachos et al., 1996), and ~ 30% at the top of the section, probably

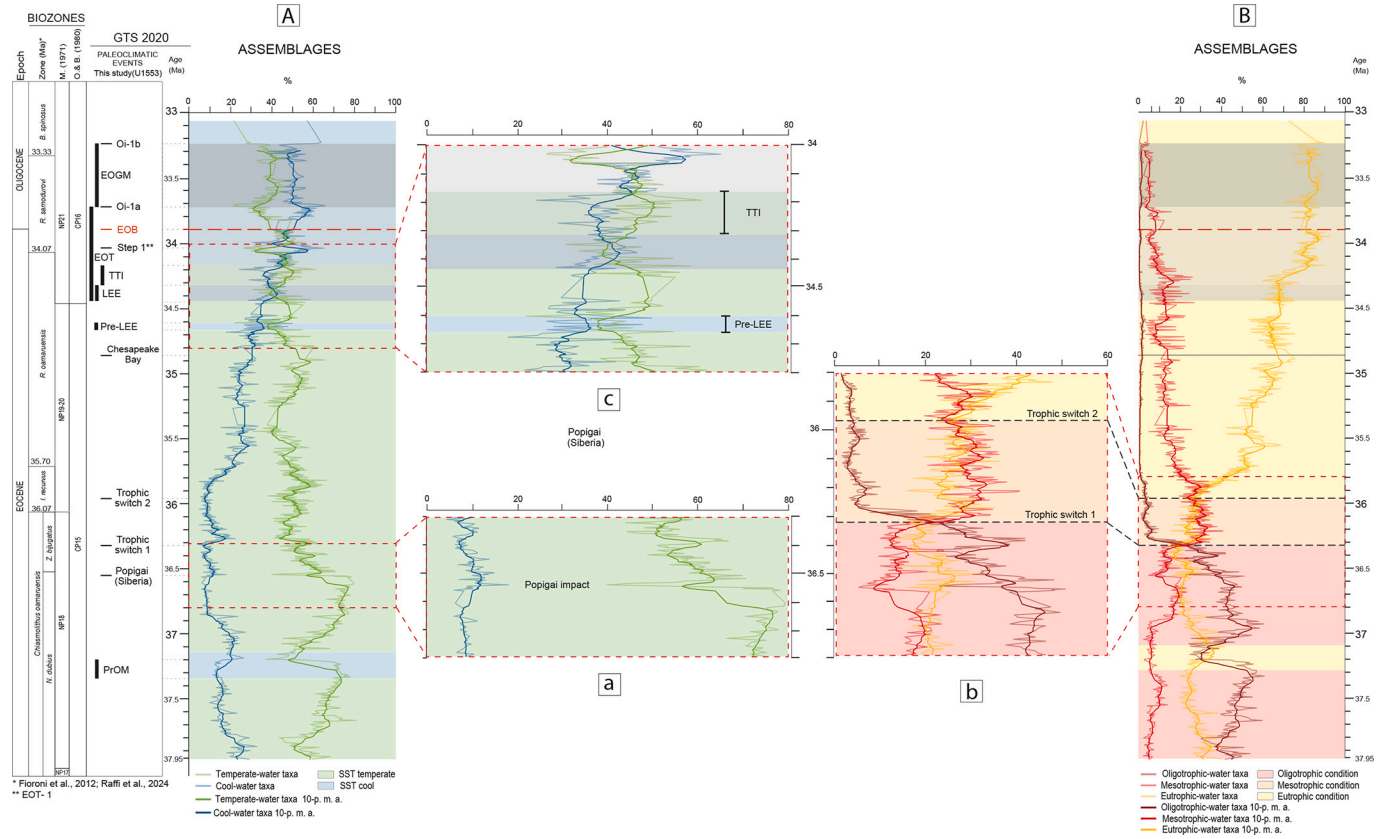

Fig. 4. Details on % assemblages during the environmental/climatic events TTI, Pre-LEE and the Popigai meteor event (references as specified in Fig. 3).

representing Oi-1b (Zachos et al., 1996). The marked cooling trend described above could probably due to an increasingly deepening of the Tasmanian Gateway and/or the Greenland-Scotland Ridge, which are considered responsible for the origination of a proto-ACC and an NCW (NADW), respectively (Abelson et al., 2008; Abelson and Erez, 2017; Coxall et al., 2018; Hutchinson et al., 2019; Straume et al., 2020, 2022). Regarding the impact of the subsequent Chesapeake Bay bolide (comet or asteroid) impact (Poag et al., 1994), that occurred at 34.86 ± 0.32 Ma (Fernandes et al., 2019), we did not observe significant short-term variations in Site U1553 temperature records (Fig. 3 A), but this could be due to the lack of samples, and data, in the corresponding interval in the section (184.78–263.81 m CCSF). However, it could be inferred that the subsequent decline in the abundance of temperate-water taxa may have been driven by an albedo feedback mechanism (Vonhof et al., 2000), which further contributed to the subsequent cooling conditions. Before the firm establishment of the cool conditions at the EOT, our record indicate a brief cooling interval from ~34.67 Ma to ~34.61 Ma (Fig. 3), referred to as "Pre-Late Eocene Event" (Pre-LEE), in which a TWWT index decrease from ~50% to ~35% and subsequent increase to values ~65% occurred. Cool-water taxa varied from values of ~20% to maximum peaks of ~50%, and temperate-water taxa varied from ~50% to ~40%, reaching minimum values of ~20% (Fig. 4 c). This possible climate event, that could correspond to the "precursor glaciation" proposed by Passchier et al. (2017) (see also Coxall et al., 2005; Katz et al., 2008), could be due to a strengthening of the proto-Ross Gyre and/or the proto-ACC or NCW (NADW) and could have caused a temporary expansion of sea ice preceding the better known Late Eocene event (LEE). During the LEE (Katz et al., 2008), cool-water taxa increased from ~30% to ~45% and temperate-water taxa decreased from ~60% to ~40% (Fig. 4 c), while the TWWT index fell from ~60% to a minimum of ~40%. This event marked the beginning of the EOT, within which we detected transient temperate interval (from ~34.31 to ~34.17 Ma), here identified as "Temperate Transition Interval" (TTI), characterized by temperate-water taxa increase to ~60% and cool-water taxa decrease to minima of ~25%, and TWWT index values of ~60% (Fig. 3, Fig. 4 c).

This proposed interstadial event could be due to an inferred temporary intrusion of warm water from the proto-Leeuwin Current through the Tasman Passage, or to a weakening of the proto-Ross Gyre, that could have triggered a flow of warm water from the EAC (East Australian Current). These regional effects affected the site under study.

Starting about 34.17 million years ago, cold-water taxa began to predominate, indicating a further cooling of surface waters, which peaked in Phase 1, the "precursor glaciation event" (Scher et al., 2011; Passchier et al., 2017; Hutchinson et al., 2021). In this phase, the increase in global ice volume was relatively minor (Lear et al., 2010; Peck et al., 2010; Pusz et al., 2011; Bohaty et al., 2012; Hutchinson et al., 2021). With the EOGM, that represented the actual glaciation as expressed by the Oi-1a and Oi-1b events (e.g., Zachos et al., 1992; Bohaty et al., 2012; Hutchinson et al., 2021), cool-water taxa further increased (from ~55% to ~66% in Oi-1a and from ~44% to ~66% in Oi-1b), and the TWWT index varied from ~40% to ~25% in Oi-1a and from ~46% to ~30% in Oi-1b (Fig. 3).

3.2.2. *Trophic conditions*

As shown in Fig. 3 B, the expected counter-correlation between oligotrophic-water taxa and eutrophic-water taxa is expressed by the value $r = -0.639$, while mesotrophic-water taxa are counter-correlated with both oligotrophic- and eutrophic-water taxa, due to their intermediate nutrient concentration preferences. We highlight key intervals in the evolving paleoecological conditions at Site U1553 that are described below.

3.2.2.1. Changes in the Late Eocene. From the base of the sequence, at ~37.95 Ma, to ~37.29 Ma oligotrophic conditions prevailed, with the abundance of oligotrophic-water taxa that fluctuated at intervals: i.e., they decreased from ~60% to a minimum of ~25% while eutrophic-water taxa increased from ~25% to ~40%, and mesotrophic-water taxa abundance remained below 10% (EI varied from ~30% to ~60%) (Fig. 3 B, C). This variability was likely linked to the PrOM climatic event, during which conditions of increased primary productivity and cooling have been argued (Scher et al., 2014; Hutchinson et al., 2021) (see sub-chapter 3.2.1). After this event, from 37.1 Ma upward, oligotrophic conditions resumed, EI decreased to values ~20% before gradually increasing again (Fig. 3 C) up to the "Trophic switch 1" (~36.31 Ma) that represents the transition to a mesotrophic phase. Just before, concomitantly with the Popigai impact event at ~36.63 Ma (Schmieder and Kring, 2020), EI increased from ~25% to ~50% and oligotrophic-water taxa temporarily decreased from ~50% to ~25% (Fig. 4 b), thus suggesting a possible response to the increase in nutrient concentrations in seawater derived by this impact (Passchier et al., 2017; Jones et al., 2019). Concomitantly with the "Trophic switch 1" a temporary increase in abundance of oligotrophic-water taxa to values ~50% was recorded before having another gradual but definitive decrease (to abundance <5%) (Fig. 4 b). Meanwhile, both mesotrophic-water taxa and eutrophic-water taxa increased from ~25% to ~30% and ~ 40%, respectively. Eutrophic conditions consistently established around ~35.96 Ma ("Trophic switch 2") and persisted until the end of the studied interval (at ~33.058 Ma). Consequently, abundance values of oligotrophic-water taxa reached very low (close to 1% - 0% values), mesotrophic-water taxa progressively decreased reaching minimum values of ~5%, while eutrophic-water taxa steadily increased reaching values up to ~90% (Fig. 3 B). Above the "Trophic switch 2", EI increased gradually and reached peaks close to 98% (Fig. 3 C). No other significant response to the climatic events mentioned in this upper interval of the section was detected by the EI and/or by changes in trophic assemblages.

Similar general trends have been documented in other high latitude successions, in which oligotrophic conditions persisted from 39.1 to 36.2 Ma (Villa et al., 2014; Sheward et al., 2024; Viganò et al., 2024). The subsequent eutrophic and cool conditions, globally spread through the Oligocene, continued until 26.5 Ma in the late Oligocene (e.g., Liebrand et al., 2017; Sheward et al., 2024; O'Brien et al., 2020).

As described above, the transition from oligotrophic to eutrophic conditions is more gradual at Site U1553 when compared with data from the Kerguelen Plateau and Maud Rise (Villa et al., 2014), and includes a mesotrophic phase in between, the reasons for explaining this pattern of change are summarized as follows:

1) the gradualness of transition observed at Site U1553 could be related to the paleobathymetry and paleotopography of the site, that could have limited the action of effective upwelling of nutrient-rich waters (see subchapters 2.3 and 3.2; Table 1; Fig. 1).
2) the gradual changes are related to the paleolatitudinal location of the site, in an area where the setting of oceanic currents fronts has probably had a different influence on sediment accumulation compared to the Kerguelen Plateau and Maud Rise areas (see

Table 1
Paleolatitudinal location and paleobathymetry of the sites considered in the present study (see Fig. 1). Data sources are from Straume et al. (2023).

SITE	PALEOLONGITUDE	PALEOLATITUDE	PALEOBATHYMETRY (m)
ODP 689D	9.670	−67.917	2159.722
ODP 744 A	85.051	−58.300	2477.056
ODP 748B	82.783	−55.309	1444.949
ODP 738B	87.329	−59.265	2454.335
IODP U1553	177.450	−55.189	4782.524
ODP 1090B	5.743	−50.938	4893.228

Table 2
Summary of interpretation of PCA results. The cool-water, temperate-water, the oligotrophic-water and eutrophic-water taxa are reported.

% ASSEMBLAGES		
EUTROPHIC-WATER TAXA	MESOTROPHIC-WATER TAXA	OLIGOTROPHIC-WATER TAXA
Chiasmolithus spp.	*Bicolumnus ovatus*	*Blackites spinosus* group
Clausicoccus subdistichus group	*Cyclicargolithus floridanus*	*Cribrocentrum reticulatum* group
Coccolithus pelagicus group	*Dictyococcites bisectus* group	*Neococcolithes dubius*
Isthmolithus recurvus	*Reticulofenestra clatrata*	
Reticulofenestra daviesii		
Reticulofenestra oamaruenesis group		
Reticulofenestra umbilicus group		
Zygrhablithus bijugatus		

% ASSEMBLAGES		
TEMPERATE-WATER TAXA		COOL-WATER TAXA
Bicolumnus ovatus	*Isthmolithus recurvus*	*Chiasmolithus* spp.
Blackites spinosus group	*Reticulofenestra clatrata*	*Clausicoccus subdistichus* group
Coccolithus pelagicus group	*Reticulofenestra oamaruenesis* group	*Neococcolithes dubius*
Cyclicargolithus floridanus	*Reticulofenestra umbilicus* group	*Reticulofenestra daviesii*
Cribrocentrum reticulatum group	*Zygrhablithus bijugatus*	
Dictyococcites bisectus group		

subchapters 2.3 and 3.2; Table 1; Fig. 1). In fact, while the sites in Kerguelen Plateau and Maud Rise could have been more subject to the effects of a "proto-AABW", the Site U1553 in Campbell Plateau was possibly more influenced by the AAIW (Zachos et al., 1992) or the SAMW (Subantarctic Mode Water), which are moderately cool and nutrient-rich currents (Sarmiento et al., 2004; Fioroni et al., 2015). It cannot be ruled out that the introduction of the mesotrophic class may explain the presence of two trophic shifts rather than one, as reported in Villa et al., 2014.

One of the consequences of global cooling during the Eocene-Oligocene could have been aridification (Dunlea et al., 2015) of Australia and Antarctica (Zachos et al., 2001a, 2001b; Wei et al., 1992). As a result, enhanced fertilisation, driven by climatic weathering of iron-rich sediments exposed on the ice-free Antarctic surface, led to an increase in eutrophic-water taxa (and increase of EI) with iron acting as a micronutrient for algal productivity (Villa et al., 2014). Alternatively, we do not rule out that the eutrophication in this area was caused or enhanced by the pulse of volcanic activity in the south-western Pacific between 42 and 35 Ma (Kennett, 1985; Dunlea et al., 2015), namely during one of five periods of explosive volcanism that began around 110 million years ago (Noble and Parker, 1974; Gardner et al., 1986; Straub and Schmincke, 1998; Carter et al., 2004). However, it is noteworthy that the sediments of IODP Exp. 329 sites, located closer to Australia as IODP U1553, show a composition close to PAAS (post-Archaean Australian shale, an iron-bearing rock; Dunlea et al., 2015) and not to a volcanic ash, taking account that PAAS is the dominant source of (iron-containing) dust in the Antarctic and South Pacific oceanic areas (Li et al., 2008). Although detailed information or ad hoc studies on the presence/concentration of iron in Site U1553 sediments are not available, Röhl et al. (2022) reported that iron was present in cores (lithologic Units II and III) corresponding to the middle Eocene-early Oligocene interval. This iron could have been originated by the same source of IODP Exp. 329 sediments, namely the PAAS from the arid Australian continent.

One final observation regarding the evolution of Site U1553 trophic conditions across the studied interval is that cool-water and eutrophic-water taxa are positively correlated ($r = 0.924$) whereas the TWWT index and the EI ($r = -0.871$) are counter-correlated. We explain this as likely due to the upwelling of cool, nutrient-rich water in the upper mixed layer (UML) of the photic zone. The cooling trend beginning followed the "Trophic switch 2" with a few hundred thousand years of delay that could be explained by biogeochemical feedback leading to substantial CO_2 sequestration, as a result of a more active biological pump in a context where environmental cofactors facilitate this cooling.

3.3. Nannofossil diversity and abundance variations

The pattern of the diversity index (Shannon index - H') of the U1553 nannofossil taxa comprises 3 phases in which diversity varies (Fig. 3 D), described as follows.

3.3.1. Phase 1 (equilibrium phase)

From the bottom of the section to the "Trophic switch 1" (from ~37.95 to ~36.31 Ma), the index is more or less constant (with a value of ~2) and suggests an "equilibrium phase" during which the oligotrophic conditions, and the presence of temperate-water taxa, persisted, except during the PrOM, when the temperate-water taxa decreased and eutrophic-water taxa increased, as indicated by the TWWT index decrease and EI increase (Fig. 3 C). However, this PrOM event does not seem to have effects on diversity, whereas a slight decrease (H' = ~1.25) is detected concomitantly to the Popigai meteor impact.

3.3.2. Phase 2 (IDH phase)

It is delineated between the "Trophic switch 1" and "Trophic switch 2" (from ~36.31 Ma to ~35.96 Ma) and labelled as "IDH phase (Intermediate Disturbance Hypothesis phase)", in which an increase of H' from ~1.5 to ~2.5 occur, indicating that oligotrophic conditions gave way to mesotrophic conditions. Also, the trend in eutrophic-water taxa and the TWWT index and EI had an average increase (Fig. 3 C), evidencing this phase. The increase could be the result of a moderate increase in nutrients and a slight mixing in the water column, that homogenized the UML and allowed the coexistence of multiple species, thereby avoiding a dominance of r-selected or K-selected species thus reflecting the so called "Intermediate Disturbance Hypothesis" (Wilson, 1994).

3.3.3. Phase 3 (decreasing phase)

The third phase extends in the interval between the "Trophic switch 2" and the top of the section (from ~35.96 to ~33.058 Ma). It is a decreasing phase in which the diversity index gradually declines from ~2.5 to ~1.5. reaching a negative peak (H' = ~1.45) concurrently with the hypothesized "pre-LEE" event. At the "Trophic switch 2" the TWWT index shows a sharp decrease and the EI a sharp increase. Within this last phase, close to ~34.2 Ma and concomitantly with the onset of cool conditions, the decreasing trend of H' becomes slightly more pronounced, with the index fluctuating from values of ~2.4 to ~0.90 (Fig. 3 D). The most oligotypic (low diversity) interval of this phase started from the EOT Step 1 and extended above. In this interval four points of pronounced reduction in H', that occur in correspondence with cool climatic events, are evident: at the onset of cool conditions (H' = ~1.25), at Step 1 (H' = ~1), at Oi-1a (H' = ~1), and at Oi-1b (H' = ~1). The TWWT index shows the same decreases while the EI does not exhibit any particular peaks. It is from phase 3 onwards that K-selected species presumably decline and R-selected species increase, as suggested by a noticeable increase in cool-water and eutrophic-water taxa (MacArthur and Wilson, 1967; Pianka, 1970; Viganò et al., 2024). To conclude, the trends that we have delineated seem to adhere with Margalef (1978) for nannoplankton, which states that maximum diversity occurs under conditions of intermediate productivity and not under conditions of high or low productivity.

As regards the evaluated total abundance of nannofossils (Fig. 3 E),

no significant trends are evident in our record, with values that range around 4000 specimen/mm^2 from the base to the top of the section. Few drastic variations occur in the interval between ~34.3 Ma and ~ 34.2 Ma, at the end of the LEE, corresponding to a considerable increase (up to ~13,000 nanno/mm^2) followed by a decrease (without a corresponding decrease in diversity/H') and a subsequent peak (up to ~11,000 nanno/mm^2) (Fig. 7). These two peaks mark the limits of the temperate interval (TTI) evidenced in this study, that preceded the onset of cool conditions. When TTI occurred, a decrease in abundance preceded a decrease in diversity (Fig. 7). A similar trend is observed through the EOGM, in which a marked decrease in abundance, at the Oi-1a onset and extended above, is not paralleled by a decrease in diversity. We explain this temporal decoupling as follows: the more cool-tolerant species (cool-water taxa) reproduced and survived, to compensate for the initial decrease in abundance of temperate-water taxa due to unfavourable environmental conditions; then, a reduction in the species diversity followed as the environmental stress persisted. The record of the reworked taxa (Fig. 3 F), that does not heavily weigh on the trend in total abundance, takes on the highest values in this interval. At ODP Sites 744 (Kerguelen Plateau) and 689 (Maud Rise), Persico and Villa (2004) documented a drastic reduction in diversity starting in the early Oligocene (~33.54 Ma). What we observed in this study is in line with the known trend of low rates of evolution and species diversity of calcareous nannofossils in the early Oligocene (Bown et al., 2004). A reduction in species diversity and abundance has been reported by several studies conducted at mid-to-low latitudes (e.g., Jones et al., 2019; Bordiga et al., 2015). In agreement with our results, Viganò et al. (2024) reported four phases of change between the end of the Eocene and the beginning of the Oligocene. Summarizing on the observed diversity and abundance variability, the general trend is delineated as a decline in K-selected species and an increase in r-selected species caused by global cooling and eutrophication during this time interval (e.g., Bordiga et al., 2015; Henderiks et al., 2022).

3.4. Paleoenvironmental controls on nannofossil assemblage during EOT–EOGM

The results of the study of Site U1553 nannofossil assemblages provide new information about the composite paleoenvironmental picture in the SO areas before and during the EOT climatic deterioration. As reported above (sub-chapter 3.2.2), similar general trends in nannofossil variability have been previously documented in other high latitude successions, and a thorough comparison of Site U1553 data with the paleoenvironmental data obtained from SO Sites ODP 689D, 748B and 738B and South Atlantic ODP Site 1090B (Figs. 5 and 6) allows us to delineate in detail differences in the records of TWWT index and EI, showing that these records evidently differ at the onset of EOT and, above all, at the EOGM. The ecological indices of the sites compared with the one under examination have not been standardised, as the EI ratio is not affected by the introduction of the mesotrophic category, whilst the TWWT index varies only to a negligible extent, since the newly characterized taxa are present with very low abundances and do not significantly (or visibly) influence the general trend. In the Site U1553 record the variability of TWWT index during the EOGM appears less extreme than in the records of sites located at higher southern paleolatitudes (ODP 689D, 738B, 744 A, 748B) (Fig. 5). This rather mild response of Site U1553 nannofossils to the EOT cooling seems to be in line with results from the record of TEX86 SST obtained at ODP Site 1172 (East Tasman Plateau; Bijl et al., 2021) and with the Mg/Ca paleothermometer from DSDP Site 277 (located in the Campbell Plateau

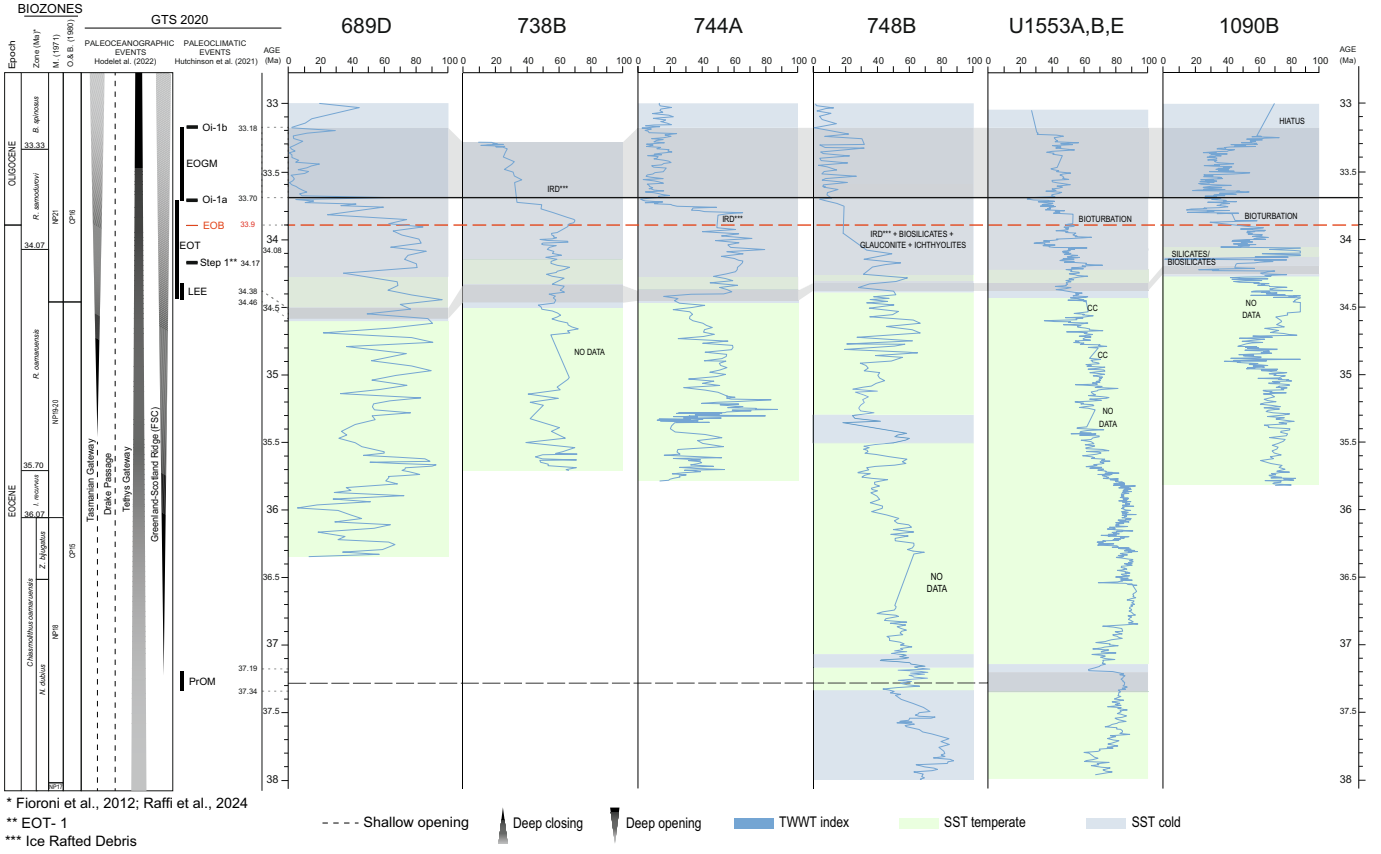

Fig. 5. Comparison of the TWWT index records of the high latitude sites considered in this study, that include: IODP Site U1553 (Campbell Plateau), ODP Sites 738B, 744 A and 748B (Kerguelen Plateau), ODP Site 689D (Maud Rise) and ODP Site 1090B (Agulhas Ridge). Data from Righi et al. (in prep.) for Site 738B; from Persico and Villa (2004) for Sites 744 A and 689D; from Villa et al. (2008) for Site 748B; from Pea (2011) for Site 1090B.

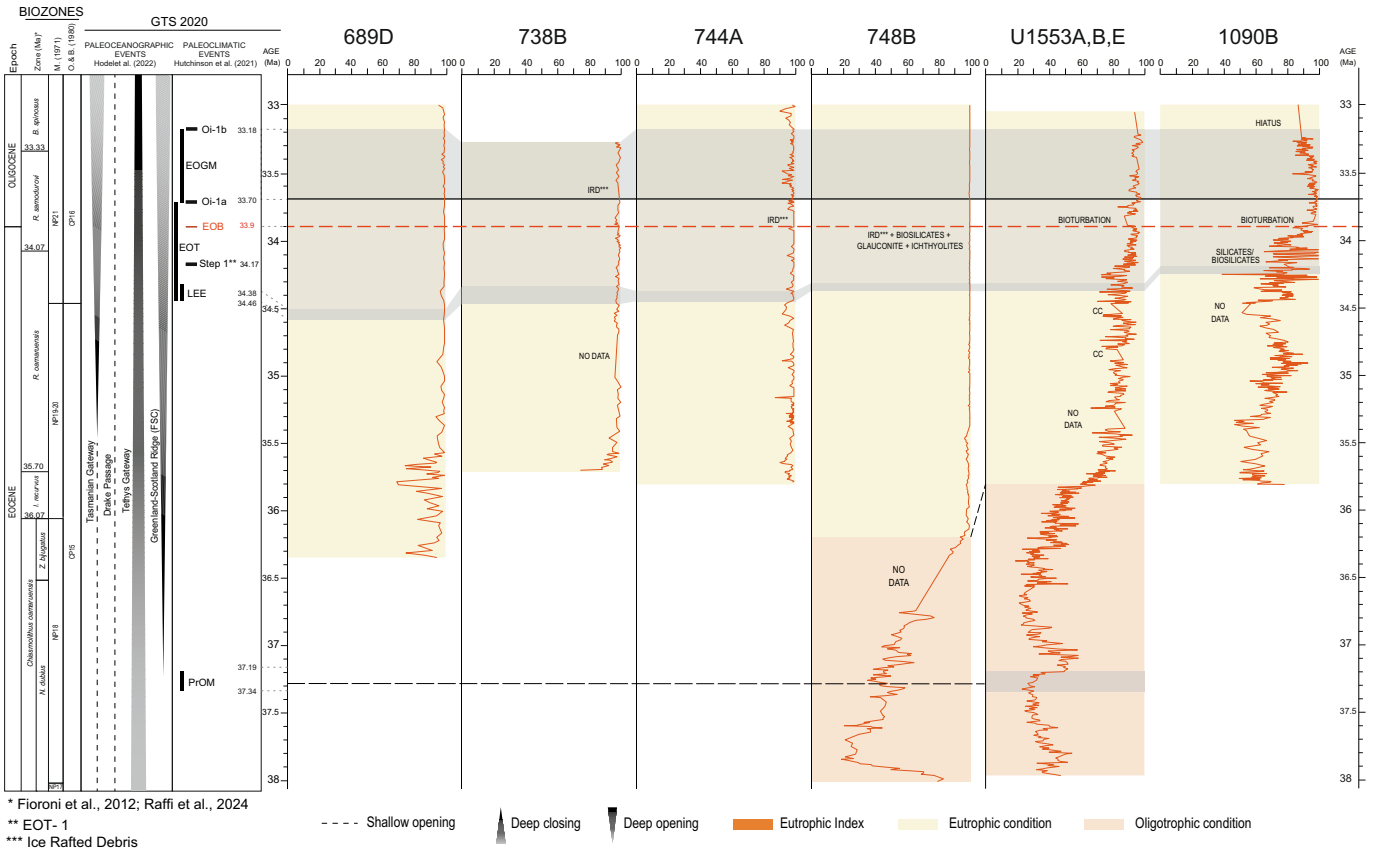

Fig. 6. Comparison of the EI records of the high latitude sites considered in this study (references as specified in Fig. 5).

as Site U1553; Hodel et al., 2022), both suggesting the absence of actual cooling at the EOT. In addition, a warming to cooling trend from late middle Eocene to the end of late Eocene was previously delineated in Site 277 sediments through the *Discoaster/Chiasmolithus* ratio (Kennett and Exon, 2004; Waghorn, 1981). These anomalous temperature reconstructions obtained in the sites from eastern Tasman Plateau and

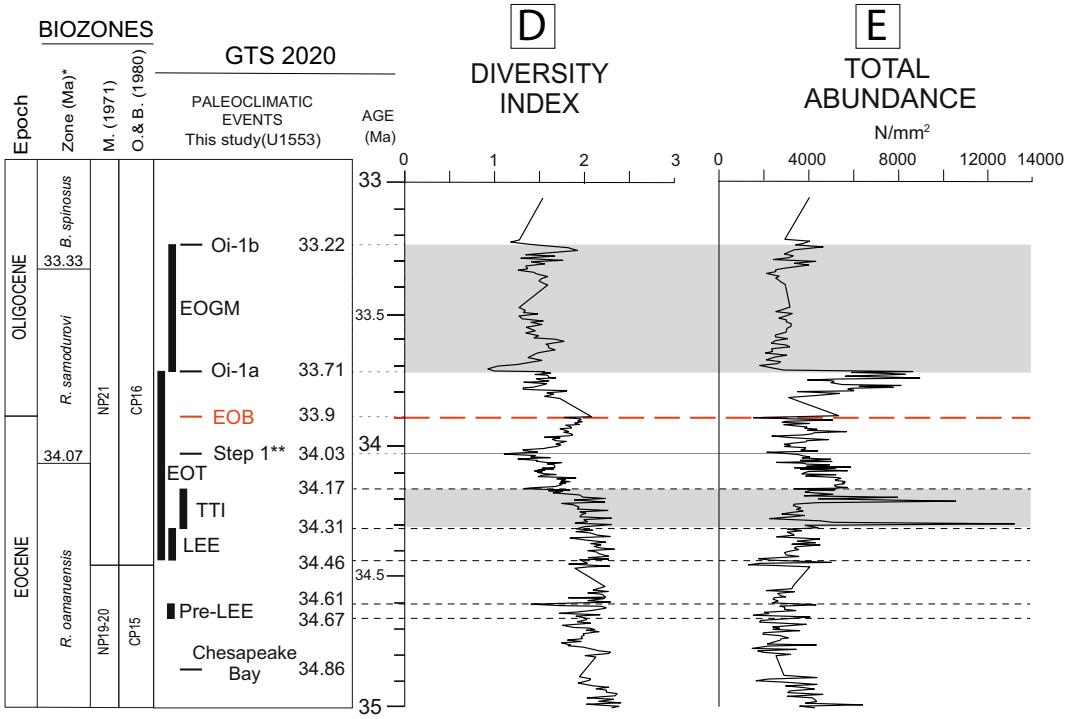

Fig. 7. Diversity index and Total Abundance records in the portion of the studied succession that corresponds to the latest Eocene and the EOT (references as specified in Fig. 3).

Campbell Plateau represent an unexpected response to the global EOT cooling phase: this anomaly could have been related to a proto-Leeuwin Warm Current flows and/or to the development of a subtropical front in the area as the Tasmanian gateway opened (or deepened) (Hodel et al., 2022).

Within the EOT interval at IODP U1553, prior to Step 1 we record a temporary increase in temperate-water taxa relative to cool-water taxa, that is evidenced by the TTI event (in the TWWT index record, Figs. 3 C, 5) and suggests a slight improvement in environmental conditions. Furthermore, during the EOGM the TWWT index remained high, as did the temperate-water taxa average abundance, reflecting a similar trend observed in the records of ODP Sites 1172 (Bijl et al., 2021; Hodel et al., 2022) and 1090B, but not so evident at the higher latitude Sites 689D, 738B, 744 A and 748B.

As a general consideration, we suggest that these differences could be related to the complex paleoenvironmental settings in the Southern Ocean/sub-Antarctic regions in the late Eocene-early Oligocene interval, thus suggesting the following reasoning:

- Firstly, the currents to the East and West of the Tasmanian Gateway were different (Fig. 1), and the positions of the sites relative to the "proto-oceanic fronts" could have triggered the upwelling of cold, nutrient-rich waters in some locations.
- Secondly, following Diester-Haass and Faul (2019), we hypothesize that differences are the result of different interaction between paleotopography and oceanic currents in the various locations.

The comparison show that higher and more constant EI values (~100) at the onset of the EOGM are those in the Site 748B record, followed by very similar values of Site 689D, while EI values appear slightly lower in the Site 738B record and more fluctuating (with values ranging between 90 and 100) in the Site 744 A record. It is noteworthy that the average EI values among the sites seem related to paleobathymetry (Table 1), namely higher values are recorded at shallow-depth locations, suggesting that this "eutrophication" related to the establishment of upwelling conditions could have been higher at lower depth locations, where upwelling turbulence was enhanced (Diester-Haass and Faul, 2019).

In the TWWT index records (Fig. 5), we note that the highest average values are recorded in Site 689D (paleolatitude of 67°S) followed by Sites 738B, 744 A, and 748 A (at paleolatitudes of 59°S, 58°S, and 55°S, respectively), which show similar slightly lower values, thus delineating a latitude gradient for nannofossil assemblage composition. This latitudinal differentiation is in accordance with the study of Wei and Wise Jr. (1990), that highlighted latitudinal gradients of calcareous nannofossils during the Eocene in the southern Atlantic.

We suggest that the main reason for the observed differences among sites could be related to the different paleoceanographic context in which the sites were located. Specifically, the Kerguelen Plateau sites, differently to the Maud Rise Site 689D, are located north of the proto-Polar Front (Fig. 1; see subchapter 3.2). Moreover, the Kerguelen Plateau could have been subject to the action of the warm flows of the proto-Leeuwin Current, which cooled down before reaching, or failed to reach, the Maud Rise due to the presence of a proto-Polar Front. In addition, locations of all these sites have probably been subjected to a proto-ACC more intensively than Site U1553 location, while the proto-ACC should not have had direct effects on Site 1090B area.

The similar paleobathymetry, that is much shallower, and the higher TWWT index and lower EI values of Sites U1553 and 1090B with respect to Sites 689D, 738B, 748B and 744 A (Table 1, Figs. 5 and 6) bring together the two sites and suggest a direct comparison between them. Factors that can have influenced their similar trends could be the following: i) at Site U1553, an influx of warm EAC waters, caused by the temporary weakening of the proto-Tasman Front (pTF), and/or the action of the warm Proto-Leeuwin current, favoured by a temporary weakening of the Proto-Ross Gyre; ii) at Site 1090B, warm water from the Agulhas Current and, possibly, from the South Atlantic Gyre (Fig. 1). In this regard, it must be pointed out that data from Site 1090B should be cautiously treated because of its location outside the South Atlantic Gyre, that promoted the upwelling conditions documented by dissolution of nannofossils and high concentration of biosilica in the sediments (Pea, 2011).

The differences in data and results between Site U1553 record and the other sites become even more evident when the climatic events/intervals highlighted in the Kerguelen Plateau (Sites 748B, 744 A) and Maud Rise (Site 689D) are taken into account, namely the "Late Eocene Climate Instability" (35.5–34.1 Ma), including the Vonhof cooling event (35.5–35.25 Ma), and the "Late Eocene Warming interval" (36.26–36.0 Ma) (Vonhof et al., 2000; Bohaty and Zachos, 2003; Persico and Villa, 2004; Jovane et al., 2006; Villa et al., 2008).

We hypothesize that, in the considered high southern latitude sections, there was a common similar response to the environmental (paleoclimatic and paleoceanographic) variability in the EOT interval, so that the observed differences between sites are not extreme and resulted from the different regional contexts of each site, as discussed above. Viganò et al. (2024), instead, suggest for nannofossil assemblages a similar response widespread at mid- and low-latitude sites in the Indo-Pacific basin, as a result of the connection between them (Fioroni et al., 2015; Jones et al., 2019; Viganò et al., 2023). Finally, all these considerations provide further evidence of a clear response from calcareous nannofossils during the climatic events of late Eocene - early Oligocene interval in the whole range of high latitude locations.

4. Conclusions

The generally well-preserved nannofossil assemblages from the continuous sedimentary succession of Site IODP U1553 allowed us to delineate and highlight the ecological preferences of taxa in this area of the SO region during the critical climatic interval encompassing the EOT. Using the data of the "Eutrophic Index" EI (Catelli et al., 2025) and the "temperate-Warm-Water-Taxa" TWWT (Villa et al., 2008) index we have been able to describe in detail the changes that occurred in a ~ 5 million years interval (from the late Eocene through the earliest Oligocene) and delineate a potential evolution of temperature (SST) and trophic conditions in the UML of these subantarctic water masses. We have detected all the signals that supposedly represent responses to the climatic/environmental events in the late Eocene, except for the "Vonhof Event". In addition, the following transient events have been evidenced:

i) The Temperate Transitional Interval (TTI), an interstadial interval within the Late Eocene (EOT) that occurred between ~34.31 and ~ 34.17 million years ago, followed the Late Eocene Event (LEE) at this site only. This event has been delineated in stable oxygen isotope data at some sites, but rarely highlighted in previous studies of nannofossil assemblages (Viganò et al., 2024; Viganò and Agnini, 2025). Given the local characterization of the TTI event, it could be attributed to paleoceanographic changes limited to a regional scale.
ii) A possible transient glaciation phase which adds to the PrOM, the brief cooling/glacial event that occurred earlier in the late Eocene. This event, named "Pre-Late Eocene Event (Pre-LEE)", occurred from ~34.67 to ~34.61 Ma within the cooling trend following the "Trophic switch 2" and was characterized by cool, eutrophic conditions. There is no mention of this event in the literature, as previously reported, it would have been triggered by regional paleoceanographic factors.
iii) The potential response of the nannofossil assemblage to the late Eocene Popigai meteor impact is tentatively proposed also for this location, although direct evidence of the impact is lacking.

As regards the EOGM, the environmental response recorded at Site

U1553 shows a different signal with respect to other sites located at high southern paleolatitudes. The latitude and location of the considered sites and their relative paleoceanographic conditions influence the differences recorded in the TWWT index at the beginning of EOGM. Sites at shallower paleodepths show higher and less fluctuating EI values suggesting that interaction between ocean currents and palaeotopographic relief resulted in a more or less significant upwelling of nutrient-rich waters (Diester-Haass and Faul, 2019). Finally, from the Shannon index (H') diversity record we suggest three subsequent phases of variability in species diversity through the late Eocene - early Oligocene interval of Site U1553, as follows: a "temperate-oligotrophic" phase (equilibrium phase), a "temperate-mesotrophic" phase (IDH phase), and a "cool-eutrophic" phase (decreasing phase). The general long-term trend shows a drastic decrease in oligotrophic-water taxa, parallel to an increase in eutrophic-water taxa, a reduction of temperate-water taxa, and an increase in cool-water taxa, albeit to a less extent than what observed in other sites at high southern paleolatitudes. The proposed interpretations help delineate an intricate environmental context in which feedback mechanisms, the various factors that trigger and modulate the EOT-EOGM and the paleoceanographic settings make the detailed reconstruction of environmental changes complex. The new nomenclature is justified by the fact that the events in U1553 are more identifiable compared to previously studied sites, and this is due to several factors: the high number of samples (809), the high sampling resolution, the continuity of the stratigraphic record, and the good preservation of the nannofossils. Although the paleoceanographic hypotheses emerging from this study cannot yet be supported by comparison with other proxies, which are currently unavailable for this site, they provide a solid foundation for future research in this area during this crucial time interval.

CRediT authorship contribution statement

Davide Righi: Writing – original draft, Methodology, Investigation, Formal analysis, Data curation. **Valentina Catelli:** Visualization, Software, Data curation. **Isabella Raffi:** Writing – review & editing. **Chiara Fioroni:** Writing – review & editing. **Giuliana Villa:** Writing – review & editing. **Davide Persico:** Writing – review & editing, Supervision.

Declaration of competing interest

The authors declare that they have no known competing financial interests or personal relationships that could have appeared to influence the work reported in this paper.

Acknowledgments

This research used samples provided by the Integrated Ocean Drilling Program (IODP), which was sponsored by the U.S. National Science Foundation (NSF) and participating countries under the auspices of the Joint Oceanographic Institutions (JOI). The work presented here benefited from the tools and framework of the COMP-R Initiative, funded by the "Departments of Excellence" program of the Ministry of University and Research (MUR, 2023-2027).

Appendix A. Appendix

Taxonomic list of the observed species.

Bicolumnus ovatus Wei & Wise, 1990.

Blackites spinosus (Deflandre and Fert, 1954) Hay & Towe (1962).

Chiasmolithus altus Bukry & Percival (1971).

Chiasmolithus eoaltus Persico & Villa, 2008.

Chiasmolithus modestus Perch-Nielsen, 1971.

Chiasmolithus nitidus Perch-Nielsen, 1971.

Chiasmolithus oamaruensis (Deflandre, 1954) Hay, Mohler & Wade (1966).

Chiasmolithus solitus (Bramlette and Sullivan, 1961) Locker, 1968.

Clausicoccus fenestratus (Deflandre and Fert, 1954) Prins, 1979.

Clausicoccus subdistichus (Roth & Hay *in* Hay et al., 1967) Prins, 1979.

Coccolithus eopelagicus (Bramlette & Riedel 1954) Bramlette & Sullivan 1961.

Coccolithus crassus Bramlette & Sullivan 1961.

Coccolithus pelagicus (Wallich, 1877) Schiller, 1930.

Coronocyclus mesostenos de Kaenel & Boesiger in Boesiger et al., 2017.

Coronocyclus nitescens (Kamptner 1963) Bramlette & Wilcoxon.

Cribrocentrum erbae Fornaciari et al., 2010.

Cribrocentrum reticulatum (Gartner & Smith, 1967) Perch-Nielsen, 1971.

Cyclicargolithus floridanus (Hay et al., 1967) Bukry, 1971.

Dictyococcites bisectus (Hay, Mohler and Wade, 1966) Bukry & Percival (1971).

Dictyococcites scrippsae Bukry & Percival (1971).

Dictyococcites stavensis (Levin and Joerger 1967).

Discoaster barbadiensis Tan Sin Hok, 1927.

Discoaster deflandrei Bramlette & Riedel, 1954.

Discoaster lodoensis Bramlette & Riedel, 1954.

Discoaster saipanensis Bramlette & Riedel (1954).

Ellipsolithus macellus (Bramlette & Sullivan, 1961) Sullivan, 1964.

Ericsonia formosa (Kamptner, 1963).

Helicosphaera bramlettei (Müller, 1970) Jafar & Martini, 1975.

Isthmolithus recurvus Deflandre (1954).

Markalius inversus (Deflandre *in* Deflandre and Fert, 1954) Bramlette & Martini, 1964.

Neochiastozygus tenansa (Deflandre in Deflandre & Fert 1954) Self-Trail 2011.

Neococcolithes dubius (Deflandre, 1954) Black (1967).

Pontosphaera duocava (Bramlette & Sullivan, 1961) Romein, 1979.

Pontosphaera pygmaea (Locker, 1967) Bystricka & Lehotayova, 1974.

Reticulofenestra clatrata Müller, 1970.

Reticulofenestra daviesii (Haq, 1968) Haq, 1971.

Reticulofenestra filewiczii (Wise & Wiegand *in* Wise, 1983) Dunkley Jones et al. 2009.

Reticulofenestra oamaruensis (Deflandre *in* Deflandre and Fert, 1954) Stradner *in* Haq (1968).

Reticulofenestra dictyoda (Deflandre *in* Deflandre & Fert, 1954) Stradner *in* Stradner & Edwards, 1968.

Reticulofenestra hillae Bukry & Percival, 1971.

Reticulofenestra oamaruensis (Deflandre *in* Deflandre and Fert, 1954) Stradner *in* Haq (1968).

Reticulofenestra samodurovi (Hay, Mohler & Wade, 1966) Roth (1970).

Reticulofenestra umbilicus (Levin, 1965) Martini & Ritzkowski (1968).

Sphenolithus moriformis (Brönnimann Y Stradner, 1960) Bramlette & Wilcoxon (1967).

Sphenolithus radians Deflandre *in* Grassé, 1952.

Umbilicosphaera detecta (de Kaenel & Villa, 1996) Young & Bown 2014.

Umbilicosphaera rotula (Kamptner, 1956) Varol, 1982.

Zygrhablithus bijugatus Deflandre in Deflandre & Fert, 1954.

Data availability

The authors confirm that all data necessary for supporting the scientific findings of this paper have been provided.

References

Abelson, M., Erez, J., 2017. The onset of modern-like Atlantic meridional overturning circulation at the Eocene-Oligocene transition: evidence, causes, and possible implications for global cooling. Geochem. Geophys. Geosyst. 18 (6), 2177–2199. https://doi.org/10.1002/2017GC006826.

Abelson, M., Agnon, A., Almogi-Labin, A., 2008. Indications for control of the Iceland plume on the Eocene-Oligocene "greenhouse–icehouse" climate transition. Earth Planet. Sci. Lett. 265 (1–2), 33–48. https://doi.org/10.1016/j.epsl.2007.09.021.

Agnini, C., Fornaciari, E., Raffi, I., Catanzariti, R., Pälike, H., Backman, J., Rio, D., 2014. Biozonation and biochronology of Paleogene calcareous nannofossils from low and middle latitudes. Newsl. Stratigr. 47, 131–181. https://doi.org/10.1127/0078-0421/2014/0042.

Aubry, M.P., 1992. Late Paleogene calcareous nannoplankton evolution: A tale of climatic deterioration. In: Prothero, D., Berggren, W. (Eds.), Eocene-Oligocene Climatic and Biotic Evolution. Princeton University Press, Princeton, N. J., pp. 272–309

Barker, P.E., Kennett, J.P., et al., 1988. Proc. ODP, Init. Repts, 113. Ocean Drilling Program, College Station, TX.

Bijl, P.K., Frieling, J., Cramwinckel, M.J., Boschman, C., Sluijs, A., Peterse, F., 2021. Maastrichtian–Rupelian paleoclimates in the southwest Pacific–a critical re-evaluation of biomarker paleothermometry and dinoflagellate cyst paleoecology at Ocean Drilling Program Site 1172. Clim. Past 17 (6), 2393–2425. https://doi.org/10.5194/cp-17-2393-2021.

Bindiu-Haitonic, R., Bălc, R., Kövecsi, S.A., Pleș, G., Silye, L., 2021. A dataset of calcareous nannoplankton and smaller benthic foraminifera from a middle Eocene nummulitic accumulation (Transylvanian Basin, Romania). Data Brief 36, 107154. https://doi.org/10.1016/j.dib.2021.107154.

Bohaty, S.M., Zachos, J.C., 2003. Significant Southern Ocean warming event in the late middle Eocene. Geology 31 (11), 1017–1020. https://doi.org/10.1130/G19800.1.

Bohaty, S.M., Zachos, J.C., Delaney, M.L., 2012. Foraminiferal Mg/Ca evidence for Southern Ocean cooling across the eocene–oligocene transition. Earth Planet. Sci. Lett. 317, 251–261. https://doi.org/10.1016/j.epsl.2011.11.037.

Bordiga, M., Henderiks, J., Tori, F., Monechi, S., Fenero, R., Legarda-Lisarri, A., Thomas, E., 2015. Microfossil evidence for trophic changes during the Eocene–Oligocene transition in the South Atlantic (ODP Site 1263, Walvis Ridge). Clim. Past 11, 1249–1270. https://doi.org/10.5194/cp-11-1249-2015.

Bown, P.R., Young, J.R., 1998. Introduction. In: Bown, P.R. (Ed.), Calcareous Nannofossil Biostratigraphy. Chapman & Hall, London, pp. 1–15. British Micropalaeontology Society Series.

Borrelli, C., Cramer, B.S., Katz, M.E., 2014. Bipolar Atlantic deepwater circulation in the middle-late Eocene: Effects of Southern Ocean gateway openings. Paleoceanography 29 (4), 308–327.

Bown, P.R., Lees, J.A., Young, J.R., 2004. Calcareous nannoplankton evolution and diversity through time. In: Thierstein, H.R., Young, J.R. (Eds.), Coccolithophores. Springer, Berlin, Heidelberg, pp. 481–508.

Bralower, T.J., 2002. Evidence of surface water oligotrophy during the Paleocene-Eocene thermal maximum: nannofossil assemblage data from ocean drilling program Site 690, Maud Rise, Weddell Sea. Paleoceanography 17 (2), 1–13. https://doi.org/10.1029/2001PA000662.

Brand, L.E., 1994. Physiological ecology of marine coccolithophores. In: Winter, J.D., Siesser, W.G. (Eds.), Coccolithophores. Cambridge Univ. Press, Cambridge, pp. 39–49.

Cappelli, C., Bown, P.R., de Riu, M., Agnini, C., 2021. The evolution of Eocene (Ypresian/Lutetian) sphenoliths: biostratigraphic implications and paleoceanographic significance from North Atlantic Site IODP U1410. Newsl. Stratigr. 54 (4), 405–431. https://doi.org/10.1127/nos/2020/0606.

Carter, L., Alloway, B., Shane, P., Westgate, J., 2004. Deep-ocean record of major late Cenozoic rhyolitic eruptions from New Zealand. N. Z. J. Geol. Geophys. 47, 481–500. https://doi.org/10.1080/00288306.2004.9515071.

Catelli, V., Persico, D., Righi, D., Raffi, I., Fioroni, C., Villa, G., 2025. Phyletic evolution of calcareous nannofossil species Reticulofenestra oamaruensis: an example of microevolution preserved at IODP Site U1553 (Southern Pacific Ocean). Mar. Micropaleontol. 196, 102452. https://doi.org/10.1016/j.marmicro.2025.102452.

Coccioni, R., Basso, D., Brinkhuis, H., Galeotti, S., Gardin, S., Monechi, S., Spezzaferri, S., 2000. Marine biotic signals across a late Eocene impact layer at Massignano, Italy: evidence for long-term environmental perturbations? Terra Nova 12 (6), 258–263. https://doi.org/10.1046/j.1365-3121.2000.00305.x.

Coxall, H.K., Pearson, P.N., 2007. The Eocene–Oligocene transition. In: Williams, M., Haywood, A.M., Gregory, F.J., Schmidt, D.N. (Eds.), Deep-Time Perspectives on Climate Change: Marrying the Signal from Computer Models and Biological Proxies. Geological Society of London, pp. 351–387. https://doi.org/10.1144/TMS002.16.

Coxall, H.K., Wilson, P.A., Pälike, H., Lear, C.H., Backman, J., 2005. Rapid stepwise onset of Antarctic glaciation and deeper calcite compensation in the Pacific Ocean. Nature 433 (7021), 53–57. https://doi.org/10.1038/nature03135.

Coxall, H.K., Huck, C.E., Huber, M., Lear, C.H., Legarda-Lisarri, A., O'Regan, M., Sliwinska, K.K., van de Flierdt, T., de Boer, A.M., Zachos, J.C., Backman, J., 2018. Export of nutrient rich Northern Component Water preceded early Oligocene Antarctic glaciation. Nat. Geosci. 11 (3), 190–196. https://doi.org/10.1038/s41561-018-0069-9.

DeConto, R.M., Pollard, D., 2003. Rapid Cenozoic glaciation of Antarctica induced by declining atmospheric CO_2. Nature 421 (6920), 245–249. https://doi.org/10.1038/nature01290.

Demircan, H., Yıldız, A., 2007. Biostratigraphy and paleoenvironmental interpretation of the Middle Miocene submarine fan in the Adana Basin (southern Turkey). Geol. Carpath. 58 (1), 41–52.

Diester-Haass, L., 1991. Eocene/Oligocene paleoceanography in the Antarctic Ocean, Atlantic sector (Maud rise, ODP Leg 113, Sites 689B and 690B). Mar. Geol. 100 (1–4), 249–276. https://doi.org/10.1016/0025-3227(91)90235-V.

Diester-Haass, L., Faul, K., 2019. Paleoproductivity reconstructions for the Paleogene Southern Ocean: a direct comparison of geochemical and micropaleontological proxies. Paleoceanogr. Paleoclimatol. 34 (1), 79–97. https://doi.org/10.1029/2018PA003384.

Diester-Haass, L., Zahn, R., 1996. Eocene-Oligocene transition in the Southern Ocean: history of water mass circulation and biological productivity. Geology 24 (2), 163–166 https://ui.adsabs.harvard.edu/link_gateway/1996Geo....24..163D/doi:10.1130/0091-7613(1996)024%3C0163:EOTITS%3E2.3.CO;2.

Drury, A.J., Westerhold, T., Wilkens, R.H., Röhl, U., 2022. Data report: splice adjustment for Site U1553. In: Röhl, U., Thomas, D.J., Childress, L.B., Expedition 378 Scientists (Eds.), South Pacific Paleogene climate. Proceedings of the International Ocean Discovery Program, 378. International Ocean Discovery Program, College Station, TX, 10.14379/iodp.proc.378.201.2022.

Dunkley Jones, T., Bown, P.R., Pearson, P.N., Wade, B.S., Coxall, H.K., Lear, C.H., 2008. Major shifts in calcareous phytoplankton assemblages through the Eocene-Oligocene transition of Tanzania and their implications for low-latitude primary production. Paleoceanography 23 (4). https://doi.org/10.1029/2008PA001640.

Dunlea, A.G., Murray, R.W., Leinen, M., Scudder, R.P., 2015. Dust, volcanic ash, and the evolution of the South Pacific Gyre through the Cenozoic. Paleoceanography 30. https://doi.org/10.1002/2015PA002829.

Fernandes, V.A., Hopp, J., Schwarz, W.H., Fritz, J.P., Trieloff, M., Povenmire, H., 2019. $^{40}Ar/^{39}Ar$ step heating ages of north American tektites and of impact melt rock samples from the Chesapeake Bay impact structure. Geochim. Cosmochim. Acta 255, 289–308. https://doi.org/10.1016/j.gca.2019.03.004.

Fioroni, C., Villa, G., Persico, D., Jovane, L., 2015. Middle Eocene-lower Oligocene calcareous Nannofossil biostratigraphy and Paleoceanographic implications from Site 711 (equatorial Indian Ocean). Mar. Micropaleontol. 118, 50–62. https://doi.org/10.1016/J.MARMICRO.2015.06.001.

Gardner, J.V., Nelson, C.S., Baker, P.A., 1986. Distribution and character of pale green laminae in sediment from Lord Howe rise: A probable late Neogene and Quaternary tephrostratigraphic record. Deep Sea Drill. Proj. Initial Rep. 90, 1145–1159.

Hallock, P., 1987. Fluctuations in the trophic resource continuum: a factor in global diversity cycles? Paleoceanography 2 (5), 457–471. https://doi.org/10.1029/PA002i005p00457.

Hammer, Ø., Harper, D.A.T., Ryan, P.D., 2001. PAST: Paleontological statistics software package for education and data analysis. Palaeontol. Electron. 4 (1), 1–9.

Henderiks, J., Sturm, D., Šupraha, L., Langer, G., 2022. Evolutionary rates in the Haptophyta: Exploring Molecular and Phenotypic Diversity. J. Mar. Sci. Eng. 10 (6), 798. https://doi.org/10.3390/jmse10060798.

Hochmuth, K., Whittaker, J., Huang, X., 2024. From bottom-water production to warm water intrusions-the cenozoic history of bottom-current evolution offshore the denman-shackleton region, East Antarctica. Paleoceanogr. Paleoclimatol. 39 (9). https://doi.org/10.1029/2024PA004948.

Hodel, F., Grespan, R., de Rafélis, M., Dera, G., Lezin, C., Nardin, E., Rouby, D., Aretz, M., Steinnman, M., Buatier, M., Lacan, F., Jeandel, C., Chavagnac, V., 2021. Drake passage gateway opening and Antarctic circumpolar current onset 31 Ma ago: the message of foraminifera and reconsideration of the Neodymium isotope record. Chem. Geol. 570, 120171. https://doi.org/10.1016/j.chemgeo.2021.120171.

Hodel, F., Fériot, C., Dera, G., De Rafélis, M., Lezin, C., Nardin, E., Rouby, D., Aretz, M., Antonio, P., Buatier, M., Steinmann, M., Lacan, F., Jeandel, C., Chavagnac, V., 2022. Eocene-Oligocene Southwest Pacific Ocean paleoceanography new insights from foraminifera chemistry (DSDP site 277, Campbell Plateau). Front. Earth Sci. 10, 998237. https://doi.org/10.3389/feart.2022.998237.

Hönisch, B., Royer, D.L., Breecker, D.O., Polissar, P.J., Bowen, G.J., Henehan, M.J., Cui, Y., Steinthorsdottir, M., McElwain, J.C., Zhang, L., 2023. Toward a Cenozoic history of atmospheric CO_2. Science 382 (6675), eadi5177. https://doi.org/10.1126/science.adi5177.

Houben, A.J., Bijl, P.K., Sluijs, A., Schouten, S., Brinkhuis, H., 2019. Late Eocene Southern Ocean cooling and invigoration of circulation preconditioned Antarctica for full-scale glaciation. Geochem. Geophys. Geosyst. 20 (5), 2214–2234. https://doi.org/10.1029/2019GC008182.

Huber, M., Brinkhuis, H., Stickley, C.E., Döös, K., Sluijs, A., 2004. Eocene circulation of the Southern Ocean: was Antarctica kept warm by subtropical waters? Paleoceanography 19 (4), PA4026. https://doi.org/10.1029/2004PA001014.

Hutchinson, D.K., Coxall, H.K., O'Regan, M., Nilsson, J., Caballero, R., de Boer, A.M., 2019. Arctic closure as a trigger for Atlantic overturning at the Eocene-Oligocene transition. Nat. Commun. 10, 3797. https://doi.org/10.1038/s41467-019-11828-z.

Hutchinson, D.K., Coxall, H.K., Lunt, D.J., Steinthorsdottir, M., De Boer, A.M., Baatsen, M., Von Der Heydt, A., Huber, M., Kennedy-Asser, A.T., Zhang, Z., 2021. The Eocene-Oligocene transition: a review of marine and terrestrial proxy data, models and model-data comparisons. Clim. Past 17 (1), 269–315. Copernicus GmbH. https://doi.org/10.5194/cp-17-269-2021.

Jones, A.P., Dunkley Jones, T., Coxall, H., Pearson, P.N., Nala, D., Hoggett, M., 2019. Low-latitude calcareous nannofossil response in the Indo-Pacific warm pool across the Eocene-Oligocene transition of Java, Indonesia. Paleoceanogr. Paleoclimatol. 34 (11), 1833–1847. https://doi.org/10.1029/2019PA003597.

Jovane, L., Florindo, F., Sprovieri, M., Pälike, H., 2006. Astronomic calibration of the late Eocene/early Oligocene Massignano section (Central Italy). Geochem. Geophys. Geosyst. 7 (7). https://doi.org/10.1029/2005GC001195.

Katz, M.E., Miller, K.G., Wright, J.D., Wade, B.S., Browning, J.V., Cramer, B.S., Rosenthal, Y., 2008. Stepwise transition from the Eocene greenhouse to the Oligocene icehouse. Nat. Geosci. 1 (5), 329–334. https://doi.org/10.1038/ngeo179.

Kennett, J.P., 1985. Minerals regime for Antarctica: Introduction. In: Alexander, L.M., Carter-Hanson, L. (Eds.), Antarctic politics and marine resources: critical choices for the 1980s, p. 172.

Kennett, J.P., Exon, N.F., 2004. Paleoceanographic evolution of the Tasmanian Seaway and its climatic implications. In: Exon, N.F., Kennett, J.P., Malone, M.J. (Eds.), The

Cenozoic Southern Ocean: Tectonics, sedimentation, and climate change between Australia and Antarctic. https://doi.org/10.1029/151GM19.
Kennett, J.P., Stott, L.D., 1990. Proteus and Proto-Oceanus: Ancestral Paleogene oceans as revealed from Antarctic stable isotopic results; ODP Leg 113. In: Barker, P.F., Kennett, J.P., et al. (Eds.), Proceedings of the Ocean Drilling Program, Scientific Results, 113B. Ocean Drilling Program, College Station, TX, pp. 865–878. https://doi.org/10.2973/odp.proc.sr.113.188.1990.
Kennett, J.P., Houtz, R.E., Andrews, P.B., Edwards, A.R., Gostin, V.A., Hajos, M., Hampton, M.A., Jenkins, D.G., Margolis, S.V., Ovenshine, A.T., Perch-Nielsen, K., 1975. Cenozoic Paleoceanography in the Southwest Pacific Ocean, Antarctic Glaciation, and the Development of the Circumantarctic Current. In: Initial Reports of the Deep Sea Drilling Project, 29. U.S. Government Printing Office. https://doi.org/10.2973/dsdp.proc.29.144.1975.
Kochhann, M., Savian, J., Tori, F., Catanzariti, R., Coccioni, R., Frontalini, F., Jovane, L., Florindo, F., Monechi, S., 2021. Orbital tuning for the middle Eocene to early Oligocene Monte Cagnero Section (Central Italy): Paleoenvironmental and paleoclimatic implications. Palaeogeogr. Palaeoclimatol. Palaeoecol. 577, 110563. https://doi.org/10.1016/j.palaeo.2021.110563.
Lasluisa, E.R., Oms, O., Remacha, E., González-Lanchas, A., Blanchar-Roca, H., Flores, J. A., 2024. Nannofossils from the Middle Eocene Sabiñánigo Sandstone Formation in the Jaca Basin (southern Pyrenees): biostratigraphy and paleoenvironmental implications. J. Micropalaeontol. 43 (1), 55–68. https://doi.org/10.5194/jm-43-55-2024.
Lear, C.H., Bailey, T.R., Pearson, P.N., Coxall, H.K., Rosenthal, Y., 2008. Cooling and ice growth across the Eocene-Oligocene transition. Geology 36 (3), 251–254. https://doi.org/10.1130/G24584A.1.
Lear, C.H., Mawbey, E.M., Rosenthal, Y., 2010. Cenozoic benthic foraminiferal Mg/Ca and Li/Ca records: toward unlocking temperatures and saturation states. Paleoceanography 25 (4). https://doi.org/10.1029/2009PA001880.
Li, F., Ginoux, P., Ramaswamy, V., 2008. Distribution, transport, and deposition of mineral dust in the Southern Ocean and Antarctica: Contribution of major sources. J. Geophys. Res. 113, D10207. https://doi.org/10.1029/2007JD009190.
Liebrand, D., de Bakker, A.T.M., Beddow, H.M., Wilson, P.A., Bohaty, S.M., Ruessink, G., et al., 2017. Evolution of the early Antarctic ice ages. Proc. Natl. Acad. Sci. 114 (15), 3867–3872. https://doi.org/10.1073/pnas.1615440114.
Liu, Z., Tuo, S., Zhao, Q., Cheng, X., Huang, W., 2004. Deep-water earliest Oligocene glacial maximum (EOGM) in the South Atlantic. Chin. Sci. Bull. 49, 2190–2197. https://doi.org/10.1007/BF03185787.
Liu, Z., Pagani, M., Zinniker, D., DeConto, R., Huber, M., Brinkhuis, H., Shah, S.R., Leckie, R.M., Pearson, A., 2009. Global cooling during the Eocene-Oligocene climate transition. Science 323 (5918), 1187–1190. https://doi.org/10.1126/science.1166368.
Livermore, R., Nankivell, A., Eagles, G., Morris, P., 2005. Paleogene opening of Drake Passage. Earth Planet. Sci. Lett. 236 (1–2), 459–470. https://doi.org/10.1016/J.EPSL.2005.03.027.
MacArthur, R.H., Wilson, E.O., 1967. The Theory of Island Biogeography.
Margalef, R., 1978. Life-forms of phytoplankton as survival alternatives in an unstable environment. Oceanol. Acta 1, 493–509.
Martini, E., 1970. Standard Tertiary and Quaternary Calcareous Nannoplankton Zonation. In: Proceedings of the 2nd Planktonic Conference, pp. 739–785. Roma.
Masaitis, V.L., Mikhailov, M.V., Selivanovskaia, T.V., 1971. Popigai Basin—An explosion meteorite crater. Doklady Akademii Nauk SSSR 197, 39–46. In Russian.
Merico, A., Tyrrell, T., Wilson, P.A., 2008. Eocene/Oligocene Ocean de-acidification linked to Antarctic glaciation by sea-level fall. Nature 452 (7190), 979–982. https://doi.org/10.1038/nature06853.
Miller, K.G., Wright, J.D., Fairbanks, R.G., 1991. Unlocking the icehouse: Oligocene–Miocene oxygen isotopes, eustasy, and margin erosion. J. Geophys. Res. Solid Earth 96 (B4), 6829–6848. https://doi.org/10.1029/90JB02015.
Monechi, S., Buccianti, A., Gardin, S., 2000. Biotic signals from nannoflora across the iridium anomaly in the upper Eocene of the Massignano section: evidence from statistical analysis. Mar. Micropaleontol. 39, 219–237.
Montanari, A., Koeberl, C., 2000. Impact stratigraphy: the Italian record. Lect. Notes Earth Sci. 93. https://doi.org/10.1007/BFb0010313. Springer-Verlag.
Nelson, C.S., Cooke, P.J., 2001. History of oceanic front development in the New Zealand sector of the Southern Ocean during the Cenozoic–a synthesis. N. Z. J. Geol. Geophys. 44 (4), 535–553. https://hdl.handle.net/10289/193.
Noble, D.C., Parker, D.F., 1974. Peralkaline silicic volcanic rocks of the Western United States. Bull. Volcanol. 38, 803–827. https://doi.org/10.1007/BF02596909.
O'Brien, C.L., Huber, M., Thomas, E., Pagani, M., Super, J.R., Elder, L.E., Hull, P.M., 2020. The enigma of Oligocene climate and global surface temperature evolution. Proc. Natl. Acad. Sci. USA 117 (41), 25302–25309. https://doi.org/10.1073/pnas.2003914117.
Okada, H., Bukry, D., 1980. Supplementary modification and introduction of code numbers to the low latitude coccolith biostratigraphy zonation (Bukry 1973, 1975). Marine Micro paleontology 51, 321–325.
Pagani, M., Huber, M., Liu, Z., Bohaty, S.M., Henderiks, J., Sijp, W., Krishnan, S., Deconto, R.M., 2011. The role of carbon dioxide during the onset of Antarctic Glaciation. Science 334 (6060), 1261–1264. https://doi.org/10.1126/science.1203909.
Pälike, H., Norris, R.D., Herrle, J.O., Wilson, P.A., Coxall, H.K., Lear, C.H., Shackleton, N. J., Tripati, A.K., Wade, B.S., 2006. The heartbeat of the Oligocene climate system. Science 314 (5807), 1894–1898. https://doi.org/10.1126/science.1133822.
Pälike, H., Lyle, M.W., Nishi, H., Raffi, I., Ridgwell, A., Gamage, K., Klaus, A., Acton, G., Anderson, Zeebe, R.E., 2012. A Cenozoic record of the equatorial Pacific carbonate compensation depth. Nature 488 (7413), 609–614. https://doi.org/10.1038/nature11360.
Pascher, K.M., Hollis, C.J., Bohaty, S.M., Cortese, G., McKay, R.M., Seebeck, H., Suzuki, N., Chiba, K., 2015. Expansion and diversification of high-latitude radiolarian assemblages in the late Eocene linked to a cooling event in the Southwest Pacific. Clim. Past 11, 1599–1620. https://doi.org/10.5194/cp-11-1599-2015.
Passchier, S., Ciarletta, D.J., Miriagos, T.E., Bijl, P.K., Bohaty, S.M., 2017. An Antarctic stratigraphic record of stepwise ice growth through the Eocene-Oligocene transition. Geol. Soc. Am. Bull. 129 (3–4), 318–330. https://doi.org/10.1130/B31482.1.
Pea, L., 2011. Eocene–Oligocene paleoceanography of the subantarctic South Atlantic: Calcareous nannofossil reconstructions of temperature, nutrient, and dissolution history, Ph.D. thesis. University of Parma, Italy (in english).
Peck, V.L., Yu, J., Kender, S., Riesselman, C.R., 2010. Shifting Ocean carbonate chemistry during the Eocene-Oligocene climate transition: implications for deep-ocean Mg/Ca paleothermometry. Paleoceanography 25 (4). https://doi.org/10.1029/2009PA001906.
Persico, D., Villa, G., 2004. Eocene-Oligocene calcareous nannofossils from Maud rise and Kerguelen Plateau (Antarctica): Paleoecological and paleoceanographic implications. Mar. Micropaleontol. 52 (1–4), 153–179. https://doi.org/10.1016/j.marmicro.2004.05.002.
Pianka, E.R., 1970. On r- and K-Selection. Am. Nat. 104 (940), 592–597. https://doi.org/10.1086/282697.
Poag, C.W., Powars, D.S., Poppe, L.J., Mixon, R.B., 1994. Meteoroid mayhem in Ole Virginny: source of the north American tektite strewn field. Geology 22 (8), 691–694. https://doi.org/10.1130/0091-7613(1994)022%3C0691:MMIOVS%3E2.3.CO;2.
Pusz, A.E., Thunell, R.C., Miller, K.G., 2011. Deep water temperature, carbonate ion, and ice volume changes across the Eocene-Oligocene climate transition. Paleoceanography 26 (2). https://doi.org/10.1029/2010PA001950.
Raffi, I., Catelli, V., Fioroni, C., Righi, D., Villa, G., Persico, D., 2024. Calcareous nannofossils from the Paleogene Southern Ocean (IODP Site U1553, Campbell Plateau). Newsl. Stratigr. 57 (4), 475–495. https://doi.org/10.1127/nos/2024/0854.
Rebesco, M., Hernández-Molina, F.J., Van Rooij, D., Wåhlin, A., 2014. Contourites and associated sediments controlled by deep-water circulation processes: state-of-the-art and future considerations. Mar. Geol. 352, 111–154. https://doi.org/10.1016/j.margeo.2014.03.011.
Röhl, U., Thomas, D.J., Childress, L.B., Anagnostou, E., Ausín, B., Borba Dias, B., Boscolo-Galazzo, F., Brzelinski, S., Dunlea, A.G., Hollis, C.J., 2022. Site U1553. https://doi.org/10.14379/iodp.proc.378.103.2022.
Salamy, K.A., Zachos, J.C., 1999. Latest Eocene–early Oligocene climate change and Southern Ocean fertility: inferences from sediment accumulation and stable isotope data. Palaeogeogr. Palaeoclimatol. Palaeoecol. 145, 61–77.
Sarmiento, J.L., Gruber, N., Brzezinski, M.A., Dunne, J.P., 2004. High-latitude controls of thermocline nutrients and low-latitude biological productivity. Nature 427 (6969), 56–60. https://doi.org/10.1038/nature02127.
Scher, H.D., Bohaty, S.M., Zachos, J.C., Delaney, M.L., 2011. Two-stepping into the icehouse: East Antarctic weathering during progressive ice-sheet expansion at the Eocene-Oligocene transition. Geology 39 (4), 383–386. https://doi.org/10.1130/G31726.1.
Scher, H.D., Bohaty, S.M., Smith, B.W., Munn, G.H., 2014. Isotopic interrogation of a suspected late Eocene glaciation. Paleoceanography 29 (6), 628–644. https://doi.org/10.1002/2014PA002648.
Scher, H.D., Whittaker, J.M., Williams, S.E., Latimer, J.C., Kordesch, W.E.C., Delaney, M. L., 2015. Onset of Antarctic Circumpolar current 30 million years ago as Tasmanian Gateway aligned with westerlies. Nature 523 (7562), 580–583. https://doi.org/10.1038/nature14598.
Schmieder, M., Kring, D.A., 2020. Earth's impact events through geologic time: a list of recommended ages for terrestrial impact structures and deposits. Astrobiology 20 (1), 91–141. https://doi.org/10.1089/ast.2019.2085.
Shannon, C.E., Weaver, W., 1949. The Mathematical Theory of Communication. University of Illinois Press.
Shepherd, C.L., Kulhanek, D.K., Hollis, C.J., Morgans, H.E., Strong, C.P., Pascher, K.M., Zachos, J.C., 2021. Calcareous nannoplankton response to early Eocene warmth, Southwest Pacific Ocean. Mar. Micropaleontol. 165, 101992. https://doi.org/10.1016/j.marmicro.2021.101992.
Sheward, R.M., Herrle, J.O., Fuchs, J., Gibbs, S.J., Bown, P.R., Eibes, P.M., 2024. Biogeochemical traits of a high latitude South Pacific Ocean calcareous nannoplankton community during the Oligocene. Paleoceanogr. Paleoclimatol. 39 (12). https://doi.org/10.1029/2024PA004946.
Straub, S.M., Schmincke, H.U., 1998. Evaluating the tephra input into Pacific Ocean sediments: distribution in space and time. Geol. Rundsch. 87, 461–476.
Straume, E.O., Gaina, C., Medvedev, S., Nisancioglu, K.H., 2020. Global Cenozoic paleobathymetry with a focus on the Northern Hemisphere oceanic gateways. Gondwana Res. 86, 126–143. https://doi.org/10.1016/j.gr.2020.05.011.
Straume, E.O., Nummelin, A., Gaina, C., Nisancioglu, K.H., 2022. Climate transition at the Eocene-Oligocene influenced by bathymetric changes to the Atlantic-Arctic oceanic gateways. Proc. Natl. Acad. Sci. 119 (17), e2115346119. https://doi.org/10.1073/pnas.2115346119.
Straume, E.O., Steinberger, B., Becker, T.W., Faccenna, C., 2023. Global Cenozoic Paleogeography and Paleo-Dynamic Topography (Version 1.0) [Dataset]. Zenodo. https://doi.org/10.5281/zenodo.8262689.
Taylor, V.E., Westerhold, T., Bohaty, S.M., Backman, J., Dunkley Jones, T., Edgar, K.M., Egan, K.E., Lyle, M., Pälike, H., Röhl, U., Zachos, J., Wilson, P.A., 2023. Transient Shoaling, Over-Deepening and Settling of the Calcite Compensation Depth at the Eocene-Oligocene transition. Paleoceanogr. Paleoclimatol. 38 (6). https://doi.org/10.1029/2022pa004493.

Thomas, D.J., Röhl, U., Laurel, C., 2018. International Ocean Discovery Program Expedition 378 Scientific Prospectus South Pacific Paleogene climate. International Ocean Discovery Program. https://doi.org/10.14379/iodp.sp.378.2018.

Tibbett, E.J., Burls, N.J., Hutchinson, D.K., Feakins, S.J., 2023. Proxy-Model Comparison for the Eocene-Oligocene transition in Southern High Latitudes. Paleoceanogr. Paleoclimatol. 38 (2). https://doi.org/10.1029/2022PA004496.

Torsvik, T.H., Steinberger, B., Shephard, G.E., Doubrovine, P.V., Gaina, C., Domeier, M., Conrad, C.P., Sager, W.W., 2019. Pacific–Panthalassic reconstructions: overview, errata and the way forward. Geochem. Geophys. Geosyst. 20 (7), 3659–3689. https://doi.org/10.1029/2019GC008402.

Viganò, A., Agnini, C., 2025. Beyond the ice: shifts in productivity and carbonate oversaturation at the Eocene–Oligocene transition. Sci. Rep. 15, 15281. https://doi.org/10.1038/s41598-025-99630-4.

Viganò, A., Coxall, H.K., Holmström, M., Vinco, M., Lear, C.H., Agnini, C., 2023. Calcareous nannofossils across the Eocene–Oligocene transition at Site 756 (Ninetyeast Ridge, Indian Ocean): implications for biostratigraphy and paleoceanographic clues. Newsl. Stratigr. 56 (2), 187–223. https://doi.org/10.1127/nos/2022/0725.

Viganò, A., Dallanave, E., Alegret, L., Westerhold, T., Sutherland, R., Dickens, G.R., Newsam, C., Agnini, C., 2024. Calcareous Nannofossils and Paleoclimatic Evolution across the Eocene-Oligocene transition at IODP Site U1509, Tasman Sea, Southwest Pacific Ocean. Paleoceanogr. Paleoclimatol. 39 (2). https://doi.org/10.1029/2023PA004738.

Villa, G., Persico, D., 2006. Late Oligocene climatic changes: evidence from calcareous nannofossils at Kerguelen Plateau Site 748 (Southern Ocean). Palaeogeogr. Palaeoclimatol. Palaeoecol. 231 (1–2), 110–119. https://doi.org/10.1016/J.PALAEO.2005.07.028.

Villa, G., Fioroni, C., Pea, L., Bohaty, S.M., Persico, D., 2008. Middle Eocene–late Oligocene climate variability: Calcareous nannofossil response at Kerguelen Plateau, Site 748. Mar. Micropaleontol. 69 (2), 173–192. https://doi.org/10.1016/J.MARMICRO.2008.07.006.

Villa, G., Fioroni, C., Persico, D., Roberts, A.P., Florindo, F., 2014. Middle Eocene to late Oligocene Antarctic glaciation/deglaciation and Southern Ocean productivity. Paleoceanography 29 (3), 223–237. https://doi.org/10.1002/2013PA002518.

Villa, G., Florindo, F., Persico, D., Lurcock, P., de Martini, A.P., Jovane, L., Fioroni, C., 2021. Integrated calcareous nannofossil and magnetostratigraphic record of ODP Site 709: Middle Eocene to late Oligocene paleoclimate and paleoceanography of the Equatorial Indian Ocean. Mar. Micropaleontol. 169. https://doi.org/10.1016/j.marmicro.2021.102051.

Vonhof, H.B., Smit, J., Brinkhuis, H., Montanari, A., Nederbragt, A.J., 2000. Global cooling accelerated by early late Eocene impacts? Geology 28 (8), 687–690. https://doi.org/10.1130/0091-7613(2000)28<687:GCABEL>2.0.CO;2.

Waghorn, D.B., 1981. New Zealand and Southwest Pacific Late Eocene and Oligocene Calcareous Nannofossils. Unpublished Ph.D. Thesis. Victoria University of Wellington.

Wei, W., Wise Jr., S.W., 1990. Biogeographic gradients of middle Eocene-Oligocene calcareous nannoplankton in the South Atlantic Ocean. Palaeogeogr. Palaeoclimatol. Palaeoecol. 79, 29–61. https://doi.org/10.1016/0031-0182(90)90104-F.

Wei, W., Villa, G., Wise Jr., S.W., 1992. Paleoceanographic implications of Eocene-Oligocene calcareous nannofossils from sites 711 and 748 in the Indian Ocean. Proc. Ocean Drill. Program Sci. Results 120, 979–999.

Westerhold, T., Marwan, N., Drury, A.J., Liebrand, D., Agnini, C., Anagnostou, E., Barnet, J.S.K., Bohaty, S.M., De Vleeschouwer, Zachos, J.C., 2020. An astronomically dated record of Earth's climate and its predictability over the last 66 million years. Science 369 (6509), 1383–1387. https://doi.org/10.1126/science.aba6853.

Wilson, J.B., 1994. The "intermediate disturbance hypothesis" of species coexistence is based on patch dynamics. N. Z. J. Ecol. 176–181. https://www.jstor.org/stable/24066772.

Wrobel, K.E., Schultz, P.H., 2003. The effect of rotation on the deposition of terrestrial impact ejecta. In: Koeberl, C., Montanari, A. (Eds.), The Late Eocene Earth: Hothouse, Icehouse, and Impacts, 452. Geological Society of America. Special Paper.

Young, J.R., Bown, P.R., Lees, J.A., 2024. Nannotax3 Website. International Nannoplankton Association. URL. www.mikrotax.org/Nannotax3.

Zachos, J.C., Kump, L.R., 2005. Carbon cycle feedbacks and the initiation of Antarctic glaciation in the earliest Oligocene. Glob. Planet. Chang. 47 (1–2), 51–66. https://doi.org/10.1016/j.gloplacha.2005.01.001.

Zachos, J.C., Breza, J.R., Wise, S.W., 1992. Early Oligocene ice-sheet expansion on Antarctica: Stable isotope and sedimentological evidence from Kerguelen Plateau, southern Indian Ocean. Geology 20 (6), 569–573. https://doi.org/10.1130/0091-7613(1992)020<0569:EOISEO>2.3.CO;2.

Zachos, J.C., Quinn, T.M., Salamy, K.A., 1996. High-resolution (104 years) deep-sea foraminiferal stable isotope records of the Eocene-Oligocene climate transition. Paleoceanography 11 (3), 251–266. https://doi.org/10.1029/96PA00571.

Zachos, J., Pagani, M., Sloan, L., Thomas, E., Billups, K., 2001a. Trends, rhythms, and aberrations in global climate 65 Ma to present. Science 292 (5517), 686–693. https://doi.org/10.1126/science.1059412.

Zachos, J.C., Shackleton, N.J., Revenaugh, J.S., Pälike, H., Flower, B.P., 2001b. Climate response to orbital forcing across the Oligocene–Miocene boundary. Science 292 (5515), 274–278. https://doi.org/10.1126/science.1058288.

Zachos, J.C., Dickens, G.R., Zeebe, R.E., 2008. An early Cenozoic perspective on greenhouse warming and carbon-cycle dynamics. Nature 451 (7176), 279–283. https://doi.org/10.1038/nature06588.

Ziveri, P., Baumann, K.-H., Bockel, B., Bollmann, J., Young, J.R., 2004. Biogeography of selected Holocene coccoliths in the Atlantic Ocean. In: Thierstein, H.R., Young, J.R. (Eds.), Coccolithophores: From Molecular Processes to Global Impact. Springer, pp. 403–428. https://doi.org/10.1007/978-3-662-06278-4_15.